NASA CR-134639
FR-6534

FINAL REPORT

EFFECT OF SWIRLING FLOW ON AUGMENTOR PERFORMANCE

By

T. R. Clements

PRATT & WHITNEY AIRCRAFT
FLORIDA RESEARCH AND DEVELOPMENT CENTER

Prepared For
NATIONAL AERONAUTICS AND SPACE ADMINISTRATION

NASA Lewis Research Center
Contract NAS3-17348

41

1. Report No.
NASA CR-134639

2. Government Accession No.

3. Recipient's Catalog No.

4. Title and Subtitle
Effect of Swirling Flow on Augmentor Performance

5. Report Date
November 1974

6. Performing Organization Code

7. Author(s)
T. R. Clements
Approved: J. H. Shadowen

8. Performing Organization Report No.
FR-6534

9. Performing Organization Name and Address
Pratt & Whitney Aircraft
Division of United Aircraft Corporation
Florida Research and Development Center
West Palm Beach, Florida 33402

10. Work Unit No.

11. Contract or Grant No.
NAS3-17348

12. Sponsoring Agency Name and Address
National Aeronautics and Space Administration
Washington, D. C. 20546

13. Type of Report and Period Covered
Contractor
June 1973-June 1974

14. Sponsoring Agency Code

15. Supplementary Notes
Project Manager; A. J. Juhasz, Air Breathing Engines Division,
NASA-Lewis Research Center, Cleveland, Ohio

16. Abstract
A test program was conducted with an augmentor which employed swirling flow as a means of promoting rapid flame propagation. The program evaluated the effect of augmentor length, swirl intensity, fuel zoning and Mach number on augmentor performance. Combustion efficiencies near 100% were demonstrated over most of the operating range which extended from an equivalence ratio of 0.2 to over 1.0. The tests were conducted at an inlet temperature of 649°C (1200°F) and at a pressure of 2 atmospheres. The augmentor total pressure losses were typical of current "state-of-the-art" augmentors.

17. Key Words (Suggested by Author(s))
Augmentor, Swirl, Swirling Flow, Afterburner, Turbojet, Exhaust Emissions, Combustion Efficiency, Pressure Loss, Exhaust Air Angle

18. Distribution Statement
Unclassified - Unlimited

19. Security Classif. (of this report)
Unclassified

20. Security Classif. (of this page)
Unclassified

21. No. of Pages
88

22. Price*

* For sale by the National Technical Information Service, Springfield, Virginia 22151

NASA-C-168 (Rev. 6-71)

FOREWORD

The research described herein was conducted by the Pratt & Whitney Aircraft Division of United Aircraft Corporation under Contract NAS3-17348 with Mr. Albert J. Juhasz of the Air-Breathing Engines, Division NASA-Lewis Research Center as Project Manager.

The period of performance for the contract was June, 1973 through June, 1974.

TABLE OF CONTENTS

PRECEDING PAGE BLANK NOT FILMED

SUMMARY

A test program has been conducted with an experimental augmentor that employed swirling flow to promote rapid flame propagation. The augmentor combustion zone was 0.381 meters (15 inches) in diameter. Three combustor cases were used giving combustor length-to-diameter ratios (L/Ds) of 0.914, 1.414 and 2.414. The swirling flow was created with swirl vanes located upstream of the fuel injection sprayrings. Three swirl vane angles were tested with nominal values of 0.44, 0.61 and 0.79 radians (25, 35 and 45 degrees).

Two fixed area, convergent exhaust nozzles were used to study the effect of Mach number on combustion efficiency. The smaller nozzle had a nominal throat diameter of 0.219 meters (8.62 inches). The larger nozzle had a nominal throat diameter of 0.272 meters (10.69 inches).

The tests were conducted at conditions simulating those of an augmented turbojet engine. The augmentor inlet temperature was 649°C (1200°F) and the combustion zone pressure was 2 atmospheres.

The demonstrated combustion efficiency was high. With the 1.414 L/D combustion zone and the 0.61 radian (35 degree) swirl vanes the combustion efficiency was near 100% at an augmentor equivalence ratio of 1.0.

The combustion efficiency was shown to be strongly dependent on the zoning of the fuel flow between the three rig fuel injection spray-rings.

The best results were obtained by gradually injecting the fuel from the outer ring to the inner ring as the fuel loading was increased.

The augmentor inlet Mach number was shown to have no effect on the measured combustion efficiency. The only exception to this was when

fuel was zoned between the outer and inner sprayings. With that fuel zoning combination the combustion efficiency was highest with the higher Mach numbers.

The augmentor cold total pressure loss was shown to be equal to that of current high performance conventional systems. At an inlet Mach number of 0.25 the total pressure loss, expressed as a drag coefficient (pressure loss/inlet dynamic head) was 0.900.

To initiate and maintain combustion, a swirling flow augmentor has an annular pilot burner surrounding the outer wall of the combustion zone. As long as the pilot is operating the mainstream flow can be ignited. Therefore, the lean blow-out was defined as the lean flammability limit of the pilot. This was determined to occur at an augmentor fuel-air ratio of 0.0007 at the 649°C (1200°F) inlet temperature.

During the course of the program combustion instabilities (rumble) in the 90 to 100 Hz range occurred. However, by proper zoning of the fuel flow between the three fuel injection zones rumble was prevented, permitting augmentor operation over the entire fuel flow range.

INTRODUCTION

Conventional augmentors are large devices. This is primarily due to the flame stabilization and propagation mechanisms employed. The flame stabilizing mechanisms consist of "vee gutters", "radial vee gutters" or combinations of these. These devices operate by creating a quiescent region in which combustion can be maintained. The flame then propagates through the unburned fuel-air mixture by turbulent eddy diffusion. It is this process that results in the rather large size of current augmentors. As the flame progresses through the unburned fuel-air mixture the resulting flame spreading angle is approximately 0.052 to 0.070 radians (3 to 4 degrees) for each flame holding device. Consequently, a large number of flame holders and considerable length are needed to spread the flame completely across the duct.

However, as the number of flame holders is increased, the augmentor total pressure losses go up. Consequently, to maintain reasonable pressure losses and combustion efficiencies a compromise is made between the number of flameholders and augmentor length. This process usually results in fairly long combustion chambers.

This method of flame stabilization and propagation has several drawbacks. First, the structure required to mount the flameholders as well as the flameholders themselves can be complicated and prone to failure. Second, the cooling of this structure is aggravated due to the high temperature of the entering air. Third, as indicated above, the combustion efficiency and also the total pressure loss vary directly with the number of flameholders. It is this trade-off between combustion efficiency and pressure loss that results in the 80 to 90 percent efficiencies of current augmentors. Fourth, the combustion efficiency is dependent on the inlet Mach number.

The swirling flow augmentor eliminates or minimizes the above problems. It operates on the principle that hot burned gases will "rise" and the colder unburned gases will sink due to the centripetal acceleration created by a strongly swirling flowfield. The beneficial effects of swirling flow were reported on over 20 years ago by I. R. Schwartz (ref. 1) who showed that combustion in a swirling flow is more stable and has less smoke than non-swirling combustion. G. D. Lewis (ref 2) has shown that flame propagation velocity in a strongly swirling flow field (centripetal accelrations 2000 to 4000 times the standard acceleration due to gravity) is controlled completely by the bouyant forces acting on the hot gases and may be as high as five times normal turbulent flame propagation velocity. The bouyancy of the hot gases is proportional to the local centripetal acceleration while the drag force is proportional to the square of the hot gas bubble velocity. By equating the bouyant and drag forces it can be shown that the hot gas bubble velocity or flame speed is given by:

$$V = C \sqrt{g_s}$$

where "V" is the flamespeed and "g_s" is the local centripetal acceleration. The value of the constant C has been determined to be approximately 1.25 as reported in reference 2. With properly designed swirl vanes, centripetal accelerations of 2400 "g's" can be generated in a .914 meter (3 foot) diameter duct at a penalty of 2 to 3 percent in total pressure. With this level of acceleration, flamespeeds of 18.6 meters per second (61 feet per second) are possible.

Because the flame spreads toward the center of rotation, combustion is initiated and maintained by an annular pilot burner surrounding the augmentor. As with conventional augmentors, there are several fuel injection zones to disperse the fuel uniformly over the duct. This concept offers several potential advantages:

1. Improved combustion efficiency due to the very high flame speeds
2. Shorter length
3. No effect on combustion efficiency due to inlet Mach number. As the Mach number increases the flame speed increases in the same proportion.
4. No need for "vee gutter" type flameholders.
5. Lower pressure drop. Also, if an increase in complexity can be tolerated, the swirl vane angle can be made adjustable. This would allow control of the swirl intensity so that only that level required for 100 percent combustion is set. This makes possible considerable reductions in total pressure loss during non-augmented and low power augmented operations. During cruise the augmentor is normally off. Therefore, with adjustable swirl vanes that can be opened fully so that no swirl is imparted to the flow significant reductions in engine total pressure losses can be made. If applied to current high performance, augmented engines this could result in a one to two percent decrease in cruise thrust specific fuel consumption.
6. Reduced exhaust emissions. Andre' Mestre (ref. 3) showed that exhaust emissions were lower with swirling flow than with non-swirling flow combustion.

The purpose of this program was to demonstrate the capability of the swirl flow augmentor concept to produce high combustion efficiencies. The tests were conducted at conditions simulating those of an augmented turbojet engine. The augmentor inlet temperature was normally 649°C (1200°F) and the total pressure was 2 atmospheres.

The program was designed to generate parametric data on the effects of swirl intensity, combustion zone length, fuel zoning and Mach number on combustion efficiency as well as locate potential problem areas. Four fuel sprayring configurations were tested in developing the final configuration. Data are presented for the final configuration only. These sprayrings were tested with all three of the originally planned swirl angle generators but with only the two shorter of the originally planned combustor lengths (L/D's of 0.914, 1.414 and 2.414).

AUGMENTOR DESIGN

The experimental augmentor used in this program is shown in figure 1. In figure 2 the rig is shown in operation at an equivalence ratio of 1.0. The 0.381 meter (15 inch) diameter of the augmentor combustion section was selected so as to be compatible with the test facility airflow and pressure capabilities.

To generate the parametric data required, several sets of rig hardware were fabricated. Among these were three swirl vane assemblies with nominal turning angles of 0.44, 0.61 and 0.79 radians (23, 35 and 45 degrees). The swirl vanes create the strongly swirling flow essential to the concept. A typical swirl vane assembly is shown in figure 3. As shown, the vanes were simple curved sheet metal vanes to minimize cost.

Three water cooled combustion chambers were available to provide combustion zone length-to-diameter ratios of 0.914, 1.414 and 2.414.

To simplify the design and reduce the cost of the rig, a fixed area convergent exhaust nozzle was used. As with the combustion chambers, the walls were water cooled. In order to study the effect of Mach number on

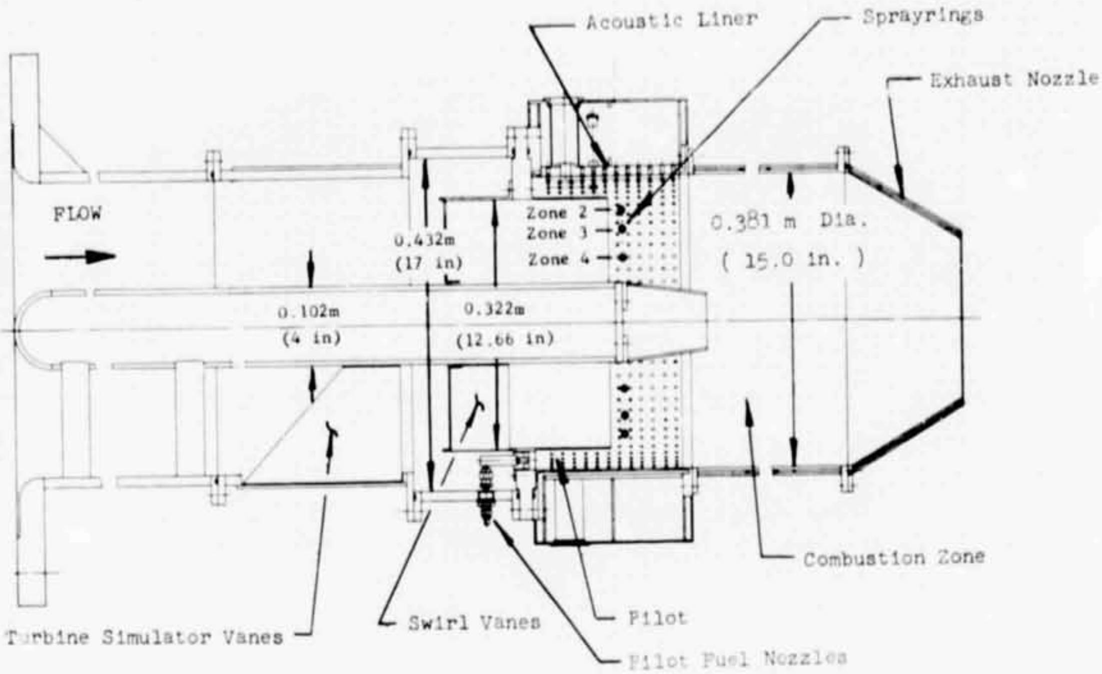

Figure 1. Swirl Augmentor Rig

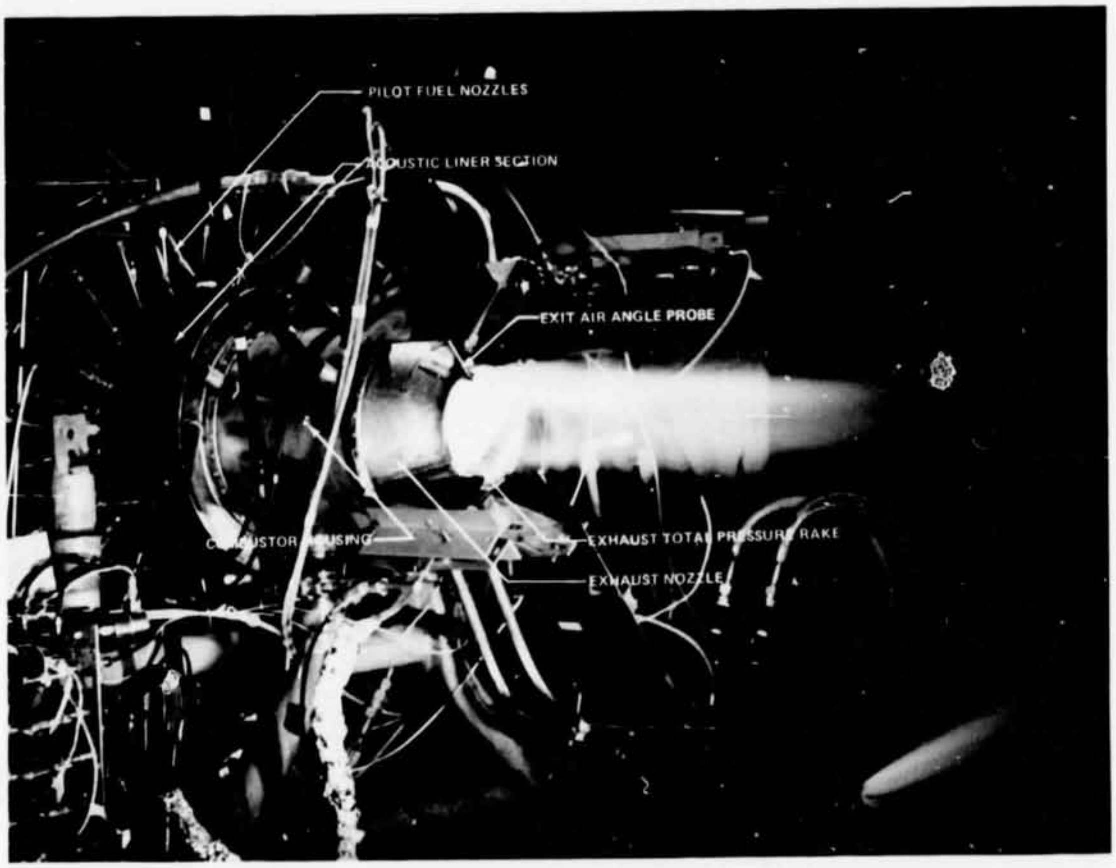

Figure 2. Experimental Swirl Augmentor Rig in Operation at an Equivalence Ration of 1.0

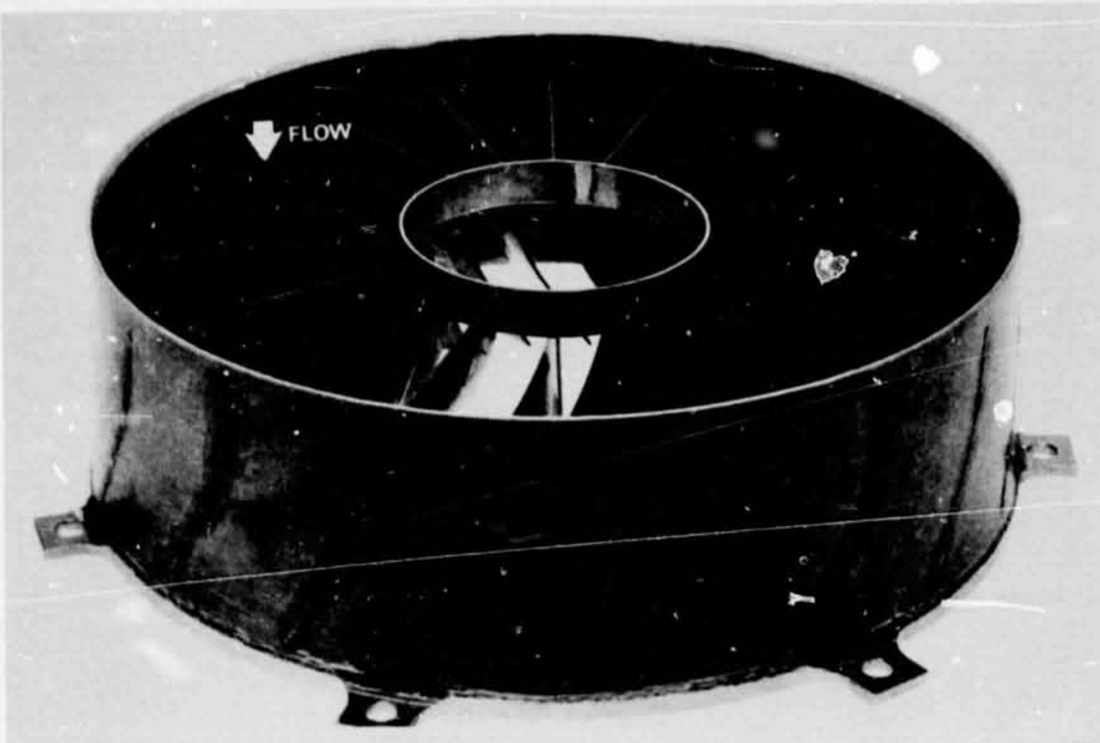

Figure 3. Typical Swirl Vane Assembly

augmentor performance, two nozzles were used. One nozzle, henceforth referred to as the small nozzle, had a nominal cold throat diameter of 0.219 meters (8.62 inches) and the other nozzle, henceforth referred to as the large nozzle, had a nominal cold throat diameter of 0.272 meters (10.69 inches).

Although the swirling flow augmentor does not require the multiple flameholders of conventional augmentors, it does require an ignition source. Since the flame spreads radially toward the rig centerline, combustion must be initiated at the outer wall. This was the function of the pilot burner shown in figure 1. The pilot burner was designed to provide a circumferentially uniform, continuous source for igniting the mainstream. Twenty fuel nozzles were equally spaced around the circumference. Because of the low pilot fuel flows, the nozzles were the air blast type in which fuel atomization is accomplished with high velocity airflows. This type nozzle with its large internal fuel passages is less sensitive to contaminated fuels. To stabilize combustion in the pilot zone, each fuel nozzle was equipped with an air swirler. All of the pilot zone air flow entered through the fuel nozzles and swirlers. Total pilot airflow was approximately 4.5 percent of the total augmentor flow.

To distribute the fuel uniformly across the duct, three concentric fuel zones were provided in the augmentor combustion chamber. The sprayrings for each zone were located at the center of equal flow areas so that each ring fed one third of the mainstream flow. Each sprayring injected fuel radially both outward and inward to provide more uniform fuel distribution. The location of the sprayrings is shown in figure 4. In the discussions that follow the outer sprayring is referred to as Zone 2. Zone 3 is the center ring and Zone 4 is the inner sprayring. Fuel from each sprayring was injected through a number of circumferentially spaced drilled orifices. Fuel atomization was enhanced by the addition of deflector tabs immediately downstream of each orifice as shown in figure 5. This design coupled with the 649°C (1200°F) inlet air temperature was considered to provide adequate fuel atomization and vaporization with considerable savings in cost. Four fuel sprayring configurations were tested in an effort to increase combustion efficiency while maintaining stable combustion at all equivalence ratios. The final configuration was tested with combustor L/D's of 0.914 and 1.414.

The acoustic liner shown in figure 1 was installed because tests conducted prior to the start of the program showed the rig to have combustion instabilities in the 500 to 1000 Hz range. The instabilities were analyzed to be the first longitudinal or first tangential mode

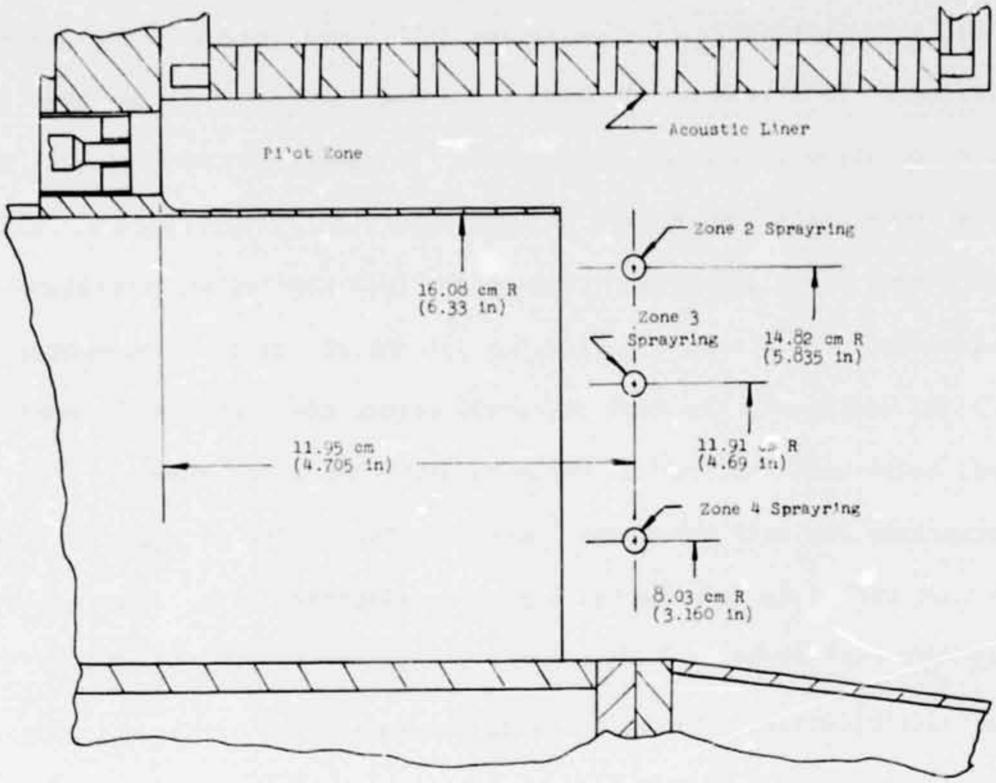

Figure 4. Location of Fuel Injection Sprayrings
(final configuration)

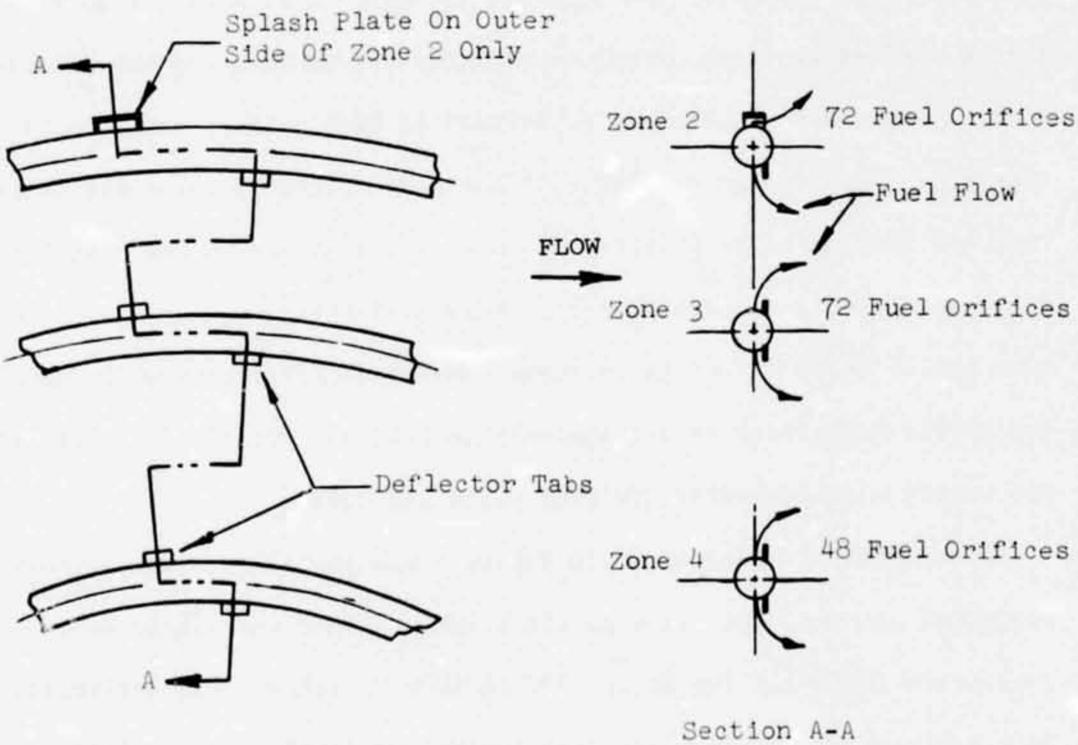

Figure 5. Fuel Sprayring Details

depending on the inlet air temperature. No attempt was made to provide a "flight type" air cooled liner as that was outside the scope of the research effort for which the rig was designed. Consequently, the hot wall was water cooled. The large backing volume of the liner provided sufficient damping even though the liner length was quite short.

The augmentor rig was designed to simulate conditions typical of turbojet or turbofan engines. The program discussed herein was designed to investigate the turbojet application, hence, the 649°C (1200°F) inlet temperature. The close proximity of the turbine and its resistance to slight downstream pressure perturbations was simulated with the turbine simulator vane assembly shown in figures 1 and 6. These vanes were simple accelerating and diffusing vanes designed to simulate the pressure drop characteristics of a turbine.

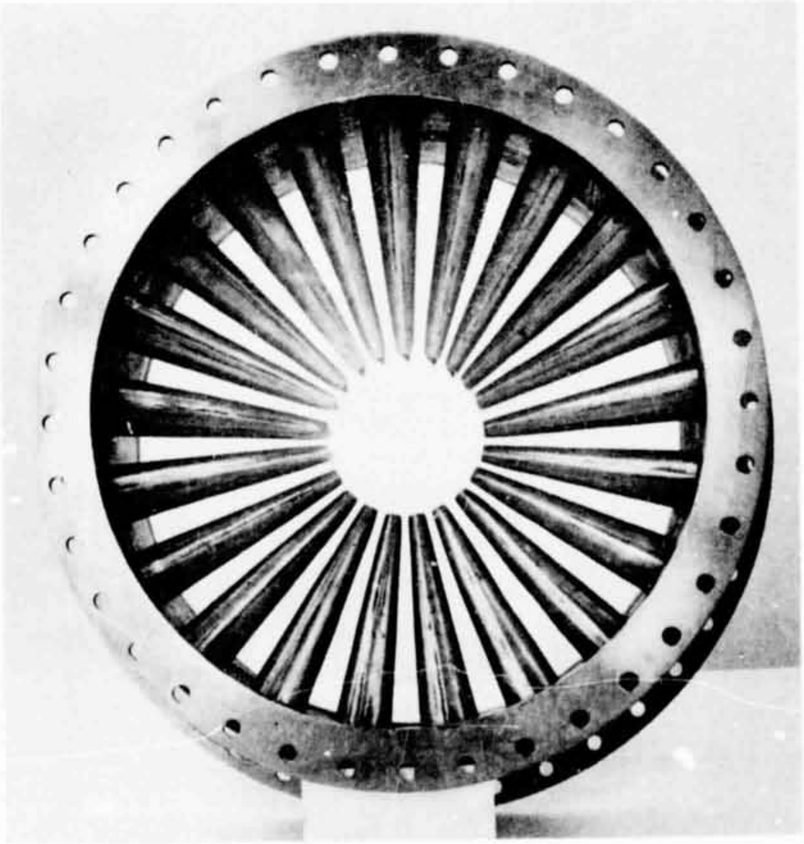

Figure 6. Turbine Simulator Vane Assembly (View looking Downstream)

TEST FACILITY

The augmentor was tested at the P&WA™ Florida Research and Development Center's B-2 component test complex. The complex consists of several test pads, a control room, an air supply and associated systems normally required for testing primary burners, augmentors and ramburners. Figure 7 shows a schematic of that portion of the facility used to test the swirl augmentor.

Test air was bled from the compressor of a J75 turbojet engine. The system can deliver 12.7 kg/sec (28 lbm/sec) airflow at pressures up to 5.516×10^5 N/M^2 (80 psia). Inlet temperatures of approximately 288°C (550°F) can be obtained at the augmentor inlet without preburning. An inline preheater is available which can raise the augmentor inlet temperature up to 871°C (1600°F).

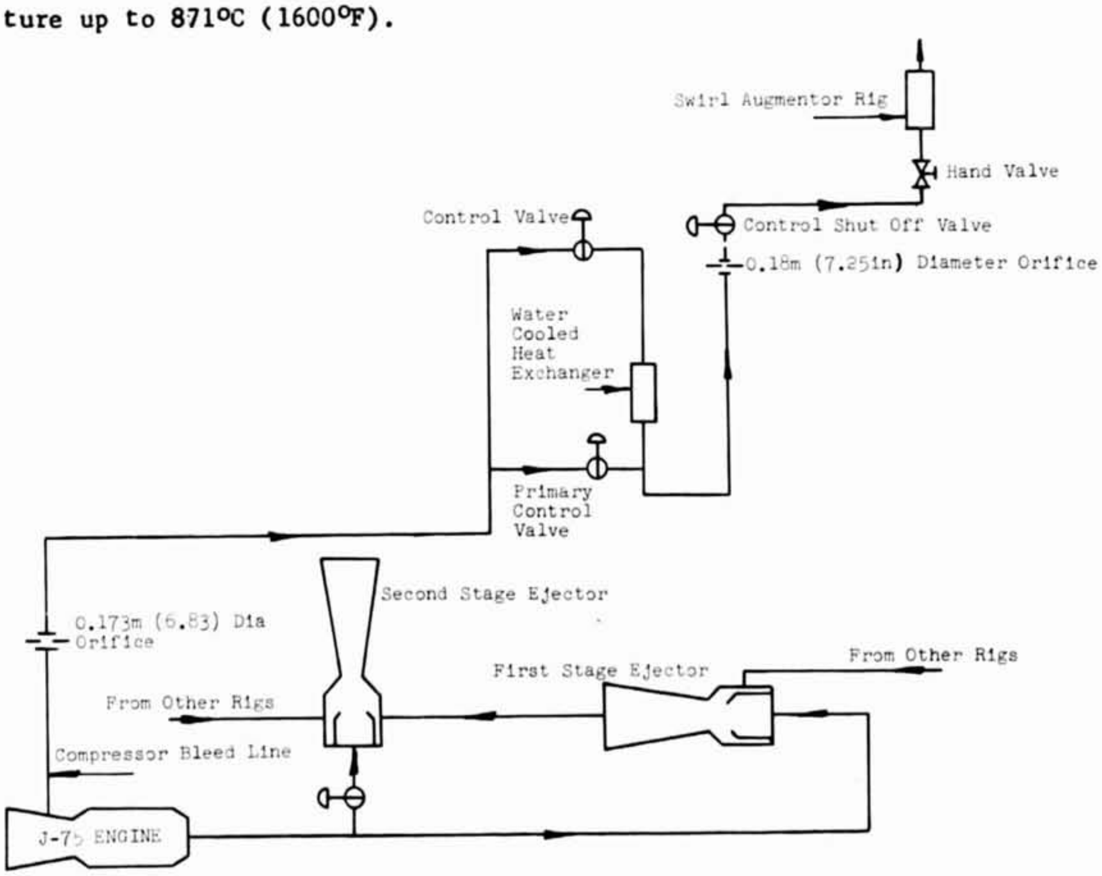

Figure 7. Test Facility Schematic

Serving the test stand is a 100-channel digital recorder capable of recording at a maximum sampling rate of 6666 samples per second. Data are recorded on magnetic tape which is directly compatible with a high-speed digital computer. Also provided are 40 channels of strip chart recorders for real-time test monitoring and a 36-channel oscillograph for higher frequency data recording.

INSTRUMENTATION

The test rig was instrumented as shown in figure 8 to provide data on rig airflow, fuel flow, augmentor inlet total pressure, combustion zone static pressure, exhaust nozzle wall temperature, air angle at the swirl vane and nozzle outlets, and the emission levels of unburned hydrocarbon, carbon monoxide and the oxides of nitrogen. The rig cooling water flowrate and inlet and outlet temperature were measured as well. These data were used to correct the combustion efficiency for heat rejected to the cooling water. The instrumentation used is briefly described in the following paragraphs.

1. Augmentor Airflow - The airflow to the rig was measured with a 0.184 meter (7.25 inch) diameter sharp-edged orifice. The orifice upstream and downstream pressures were measured with flange static pressure taps. The air temperature was measured with two chromel-alumel thermocouples located downstream of the orifice. In case the instrumentation on this orifice should fail a back-up 0.173 meter (6.83 inch) diameter orifice was available to measure rig airflow. The instrumentation on that orifice was similar to that of the primary orifice.

2. Augmentor Fuel Flow - The fuel flows to the preheater, pilot and zones 2, 3 and 4 were measured with turbine type flow meters.

3. Preheater Inlet Air Temperature - This temperature was measured

with two, shielded chromel-alumel thremocouples.

4. Augmentor Inlet Total Pressure - The augmentor inlet total pressure was measured with two Kiel type total pressure probes.

5. Augmentor Inlet Total Temperature - The augmentor inlet total temperature was taken as the ideal preheater outlet temperature. See Appendix A, paragraph 30. However, as figure 8 shows, the augmentor inlet total temperature was also measured directly with seven chromel-alumel thermocouples.

6. Combustion Zone Static Pressure - The static pressure in the combustion zone was measured with two wall taps located immediately upstream of the exhaust nozzle.

7. Exhaust Nozzle Total Pressure - The total pressure at the exhaust nozzle was normally calculated by an iterative procedure using the nozzle inlet and throat geometric areas, the augmentor mass flow and the combustion zone static pressure at the nozzle inlet. See Appendix A, paragraph 38. For most of the tests, however, this procedure was supplemented with a direct measurement of total pressure with a multi-point rake, see figure 8.

8. Exhaust Nozzle Wall Temperature - The wall temperature of the exhaust nozzle was measured with four chromel-alumel thermocouples located at the nozzle throat and equally spaced around the circumference. These data were used to correct the nozzle throat diameter for thermal expansion.

9. Cooling Water Flowrate - The cooling water flowrate to the rig was measured with a 0.031 meter (1.225 inch) diameter sharp edged orifice located in the discharge manifold. The orifice was equipped with flange static pressure taps.

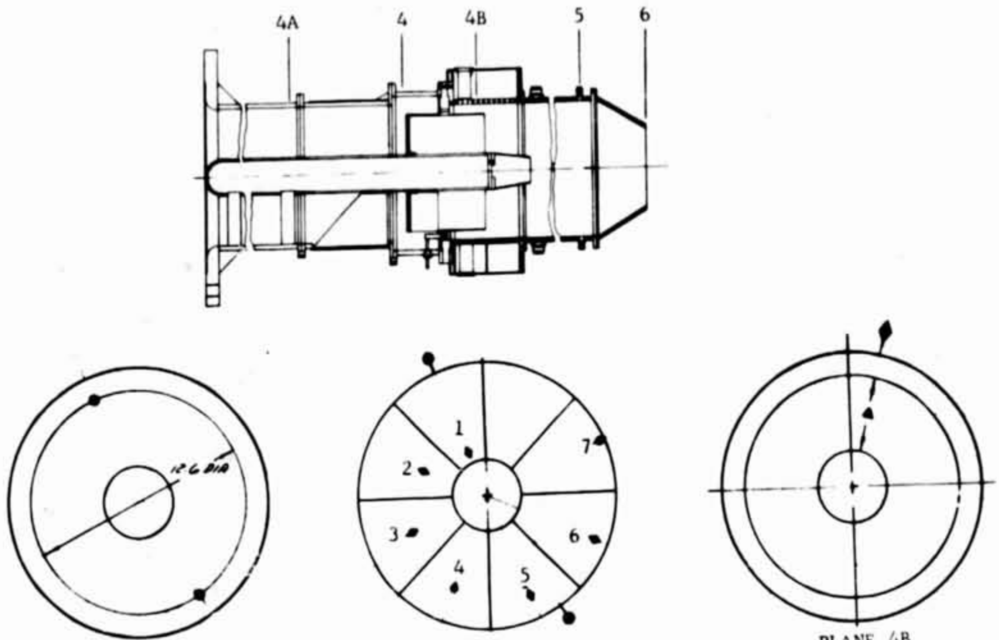

PLANE 4
Swirl Vane Inlet

PLANE 4A
Turbine Simulator Vane Inlet

PLANE 4B
Swirl Vane Discharge

Temperature Probe	Radial Position
1	7.06cm (2.78 in)
2	9.91cm (3.90 in)
3	12.09cm (4.76 in)
4	13.94cm (5.49 in)
5	15.57cm (6.13 in)
6	17.04cm (6.71 in)
7	13.42cm (7.25 in)

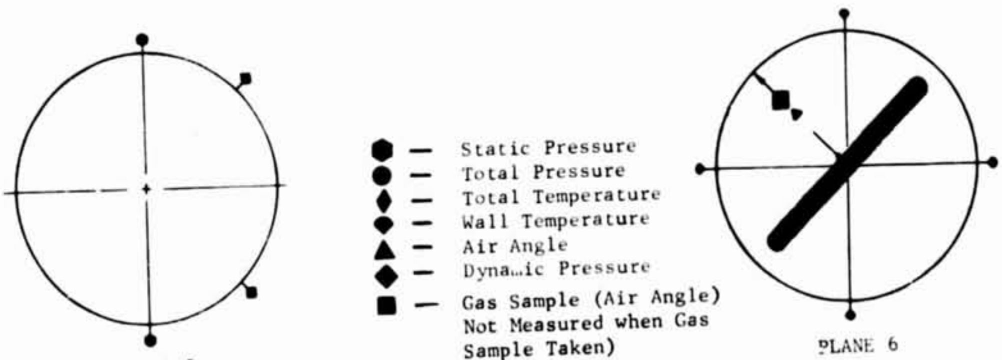

PLANE 5
Nozzle Inlet

PLANE 6
Nozzle Exit
Total Pressure Rake Installed at this Location, however, Data were not used.

Figure 8. Basic Rig Instrumentation

10. Cooling Water Temperature - The inlet and outlet cooling water temperatures were measured with chromel-alumel thermocouples. The inlet thermocouple was located in the supply manifold. The outlet thermocouple was located in the discharge manifold just upstream of the waterflow orifice.

11. **Air Angle- The air angles at the swirl vane and exhaust nozzle discharge were measured with self-balancing air-angle probes. At the swirl vane discharge the air angle was measured with the probe shown in figure 9 and at the exhaust nozzle exit the probe shown in figure 10 was used to measure the air angle. The probes were traversed in the radial direction from the outer radius to the rig centerline.**

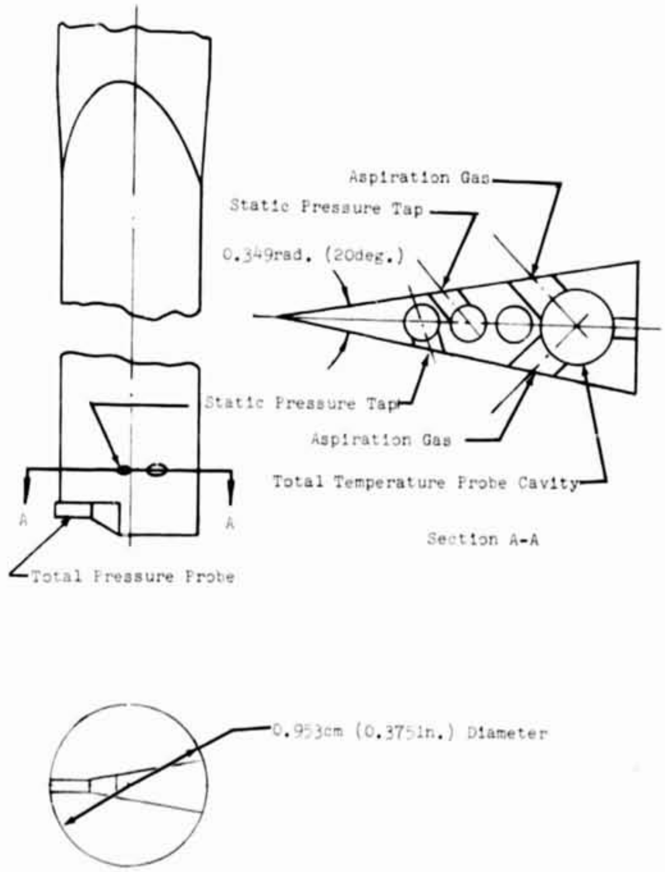

Figure 9. Air Angle Probe used at the Swirl Vane Discharge

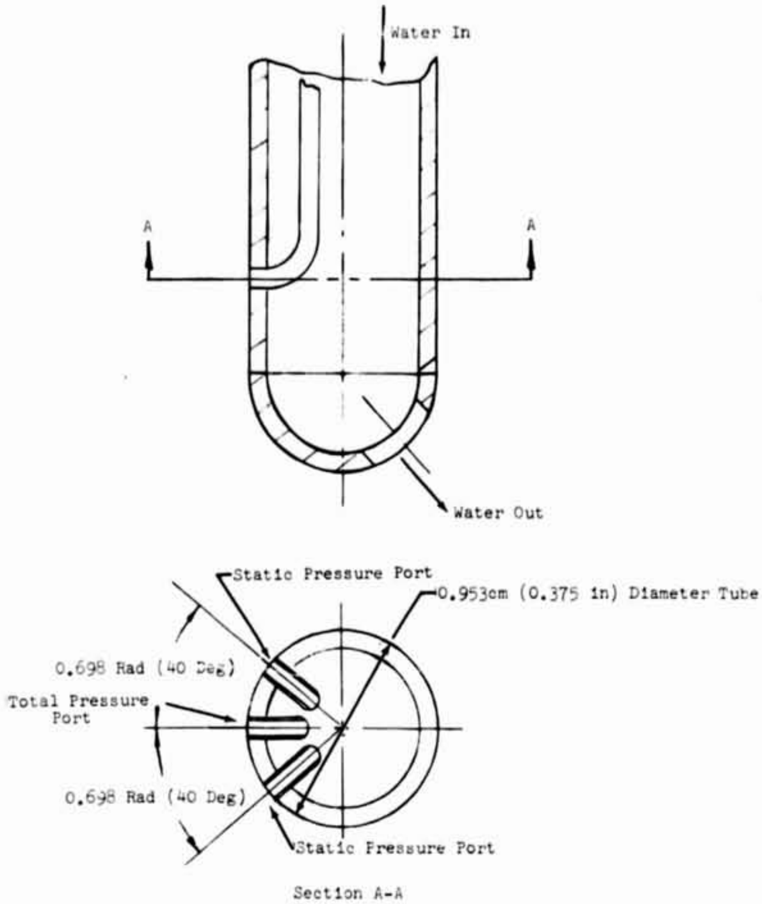

Figure 10. Air Angle Probe used at the Nozzle Exit (Drawing Courtesy of the NASA-Lewis Research Center)

12. **Hydrocarbon Emissions - The emission level of unburned hydrocarbon was determined with an F.I.D. (flame ionization detector) analyzer. The sample gas was transferred to the analyzer through electrically heated lines to maintain its temperature above 149°C (300°F). The sample was obtained with a single point probe, figure 11, which was traversed across the nozzle exit from the rig centerline to the outer radius. Samples were obtained at five points located on equal area centers.**

13. **Carbon Monoxide Emissions - The emission level of carbon monoxide was determined with an NDIR (non-dispersive infrared) analyzer.**

14. **Nitrogen Oxide Emissions - The emission level of the oxides of nitrogen were measured with a chemiluminescent analyzer.**

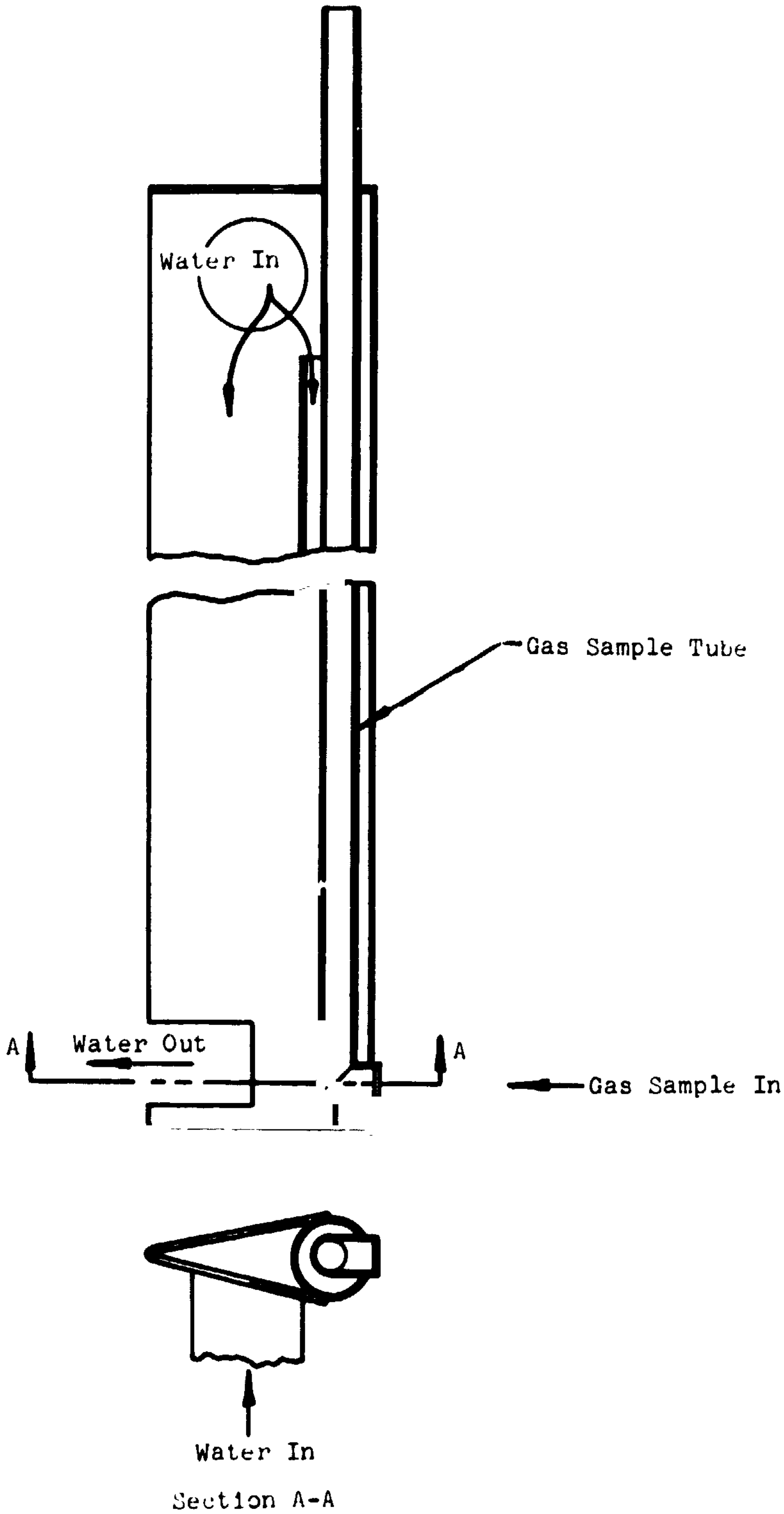

Figure 11. Gas Sampling Probe

EXPERIMENTAL PROCEDURE

The swirl augmentor was tested at a near constant pressure of 2 atmospheres over the full range of equivalence ratios investigated. With the small nozzle installed, the augmentor was brought on line by first increasing the airflow and preheater fuel flow until the exhaust nozzle was choked and an inlet temperature of 649°C (1200°F) was set. The pilot burner was then ignited at a local equivalence ratio of 1.0 using an automotive type spark plug. The pilot was maintained at an equivalence ratio of approximately 1.0 during the remainder of the test. The various rig fuel zones were brought on line by simply setting the fuel flow desired. Ignition was accomplished with the pilot burner. Minimum fuel flow to each zone was approximately 90.7 Kg/Hr (200 pph). This was required to stay above the lower operating limit of the turbine type flow meters.

With the large nozzle installed the start up procedures had to be modified. At the 649°C (1200°F) inlet temperature condition the airflow required to choke the large nozzle was greater than the facility capability. Therefore, an initial airflow of approximately 9.0 Kg/sec (20 lbm/sec) was set. The pilot burner was ignited as before and an equivalence ratio greater than 0.2 was set on one of the augmentor fuel zones. With the increased nozzle outlet temperature the nozzle could be choked within the airflow capacity of the facility.

Since the desired test condition was 2 atmospheres inlet pressure and 649°C (1200°F) inlet temperature the airflow and preheater fuel flow had to be adjusted whenever the augmentor equivalence ratio was altered. This results from using a fixed area exhaust nozzle. Figure 12 shows the relation between the swirl vane inlet Mach Number and the augmentor equivalence ratio with both the small and large nozzles at the 2 atmosphere test condition assuming 100% combustion efficiency.

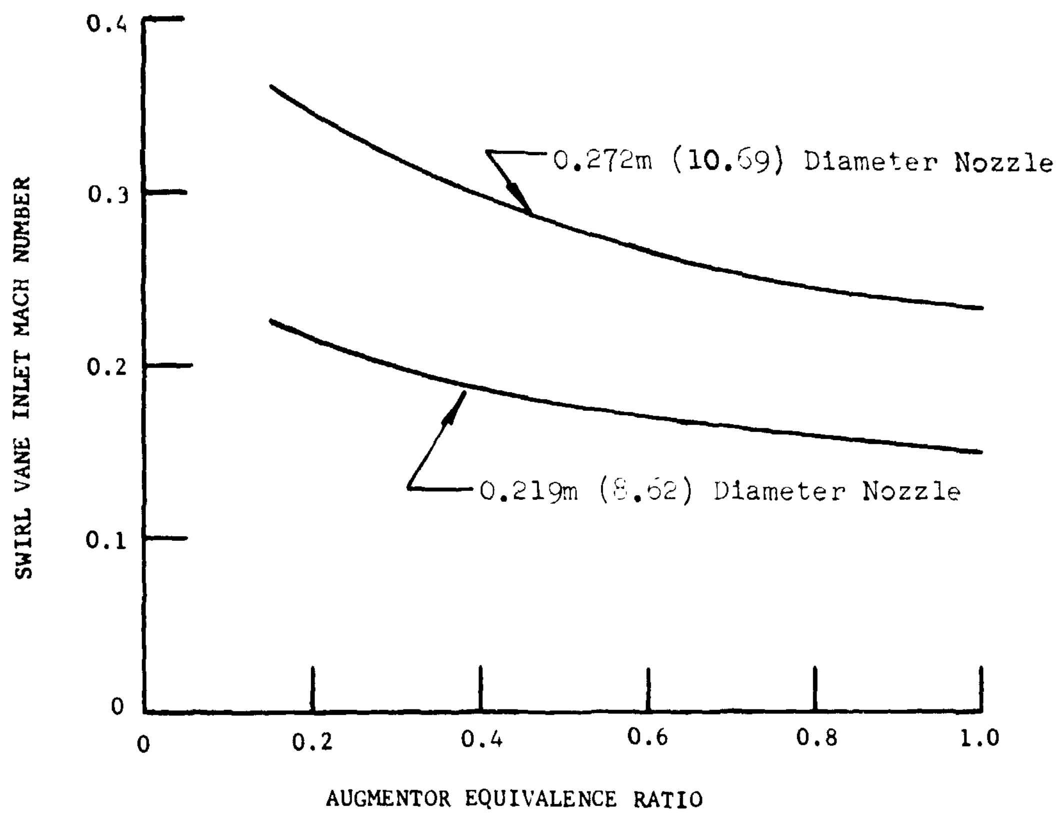

Figure 12. Variation of Swirl Vane Inlet Mach Number with Augmentor Equivalence Ratio

All of the data with the exception of the gas sampling data were recorded using a high speed digital recording system. Between desired test points the recording system was operated at a recording speed of 1 scan/sec which means that all of the data channels were recorded one time each second. When a test point was set, however, the recording speed was increased to 10 scans/sec and data were recorded over a five second interval. These 50 readings were subsequently averaged to provide a good value for each data channel.

In the program the combustion efficiency was determined by gas sampling and by the "choked nozzle method". With the "choked nozzle method," if the mass flow, total pressure, and nozzle geometric area and discharge coefficient are known the exhaust temperature and hence combustion efficiency can be determined. The nozzle discharge coefficient was determined by choking the nozzle during cold flow so that an isothermal temperature field existed at the nozzle. The mass flow and nozzle total pressure were then measured and the nozzle discharge coefficient determined using the effective area determined from the measured values of mass flow, total pressure and temperature and the known goemetric area. This was done for the small nozzle using all three swirl vane assemblies and also without any swirl. With the large nozzle, however, the inlet air temperature had to be raised to over 92.°C (1700°F) with the preheater in order to choke the nozzle with the available airflow rate. This presented a high risk of damaging uncooled portions of the rig immersed on the gas stream. Consequently only one calibration point using the 0.61 rad (35 deg) swirl vanes was obtained.

The gas sampling equipment was calibrated in accordance with the Society of Automotive Engineers Specification ARP 1256.

CALCULATIONS

The basic performance calculations are presented in the following paragraphs. For a more complete description of the performance calculation procedure see Appendix A.

Combustion Efficiency - The augmentor combustion efficiency is normally given by:

$$EFFMB = 100 \left[\frac{TT6 - TT4A}{TT6IDEAL - TT4A} + \frac{3600\ Qloss}{4.273 \times 10^{7}\ WFT} \right]$$

where

EFFMB	=	augmentor combustion efficiency, %
TT6	=	actual outlet total temperature, °C (°F)
TT6IDEAL	=	ideal outlet total temperature, °C (°F)
TT4A	=	inlet total temperature, °C (°F)

Qloss = heat rejected to combustion chamber jacket cooling water, Joules/sec (BTU/sec)

WFT = augmentor fuel flow, Kg/Hr (pph)

The heating value of the JP-5 kerosine fuel was taken as 4.273×10^7 Joules/kg (18370 BTU/lbm).

For a portion of the testing this method of determining combustion efficiency was supplemented by a second method based on analysis of the exhaust products. By determining the amount of unburned hydrocarbons and carbon monoxide still present in the gases passing throu[illegible] nozzle the combustion efficiency can be determined from:

$$EFFMB = 100 - 100 \left[\frac{HVco\ (CO) + HVf\ (UHC)}{HVf \times 10^3} \right]$$

where

EFFMB = augmentor combustion efficiency, %

CO = emission index of carbon monoxide

UHC = emission index of unburned hydrocarbons

HVco = heating value of carbon monoxide = 1.010×10^7 Joules/kg (4343 BTU/lbm)

HVf = heating value of the fuel = 4.273×10^7 Joules/hg (18370 BTU/lbm)

Total Pressure Loss - The augmentor total pressure loss is given by:

$$DPAUG = 100 \left[\frac{PT4A - PT6A}{PT4A} \right]$$

where

DPAUG = augmentor total pressure loss (percent)

PT4A = inlet total pressure , N/m^2 (psia)

PT6A = outlet total pressure , N/m^2 (psia)

Swirl Vane Mach Number - The swirl vane Mach Number is the Mach Number of the flow as it enters the swirl vanes. It is given by:

$$M4 = \left[\frac{(Wa)\ (1 + HUM + FAPH)\ SVFR}{PT4A\ (A_4)}\right] * \sqrt{\frac{R4(TT4A)}{G(GAM4)}\ \left(1 + \frac{GAM4-1}{2}\ M4^2\right)^{\frac{GAM4+1}{GAM4-1}}}$$

where

M4	= swirl vane inlet Mach Number
Wa	= augmentor dry airflow , Kg/sec (lbm/sec)
SVFR	= fraction of total mass flow passing through the swirl vanes
HUM	= specific humidity
FAPH	= preheater fuel-air ratio
PT4A	= inlet total pressure , N/m^2 (psia)
A4	= swirl vane inlet area = 0.0729 m^2 (113 in^2)
GAM4	= gas specific heat ratio
R4	= gas constant at swirl vane inlet
G	= standard acceleration due to gravity

Swirl Intensity - The nominal swirl intensity at the pilot zone inner wall expressed in terms of the standard gravitational constant or "g's" is:

$$g_s = (V4\ TAN\ \alpha)^2 / (RG)$$

where

g_s	= swirl intensity in "G's"
V4	= swirl vane inlet velocity ; m/sec
α	= swirl vane turning angle , radians (degrees)
R	= pilot zone inner wall radius , meters (feet)
G	= standard acceleration due to gravity

RESULTS AND DISCUSSIONS

A swirling flow augmentor was tested at conditions simulating those encountered in an augmented turbojet engine. The augmentor inlet temperature and pressure were 649°C (1200°F) and 2 atmospheres respectively. The effects of swirl intensity, combustion zone length, fuel zoning and augmentor inlet Mach Number on augmentor performance was determined. Table I summarizes the data obtained during the program.

A. Combustion Efficiency

In general, the combustion efficiency was high. By proper fuel zoning the data show that combustion efficiencies near 100 percent could be obtained at equivalence ratios up to 1.0.

Two methods were used to calculate the combustion efficiency. The first was the so-called "choked nozzle method". By knowing the mass flow, total pressure, nozzle geometric area and discharge coefficient the total temperature of the gases passing through the nozzle and, hence, combustion efficiency could be calculated.

The second method calculates combustion efficiency by determining the amount of unburned hydrocarbons and carbon monoxide still present in the gases passing through the nozzle. In the discussion that follows the choked nozzle data are first discussed. They are then compared to the efficiency data obtained by sampling the exhaust for unburned hydrocarbons and carbon monoxide.

The data of figure 13 show the effect of increasing the length-to-diameter ratio from 0.914 to 1.414. The data were obtained using the 0.219 meter (8.62 inch) diameter exhaust nozzle and the 0.61 radian (35 degree) swirl vanes with both combustor L/D's. In general, with the

TABLE I. Test Summary

Run No.	Point No.	α RAD	α DEG	L/D	Wa kg/sec	Wa lbm/sec	PT4A N/M² 10⁻³	PT4A PSIA	TT4A °C	TT4A °F	M4	Mref	Vref m/sec	Vref ft/sec	Swirl g's	DPSV %	DPMOM %	DPAUG %	CDAUG	F/A	∅	∅1	∅3	∅4	TT6 °C	TT6 °F	EFFMB %	EFFMB Gas Sample
23.01	1102	0.61	35	1.414	7.775	17.14	221.5	32.13	646	1195	0.214	0.153	89.3	293	4756	4.34	0.75	5.09	1.71	0.0126	0.218	0.169	-	-	923	1694	79	-
23.01	1415	0.61	35	1.414	6.913	15.24	220.1	31.92	656	1213	0.192	0.137	80.8	265	3880	3.21	1.19	4.40	1.84	0.023	0.404	0.348	-	-	1222	2232	87	-
23.01	1802	0.61	35	1.414	6.260	13.80	216.8	31.44	659	1218	0.176	0.126	74.7	245	3317	2.30	1.52	3.82	1.89	0.042	0.722	0.660	-	-	1449	2640	73	-
23.01	2098	0.61	35	1.414	6.455	14.23	218.8	31.74	666	1231	0.181	0.129	76.8	252	3510	2.51	1.32	3.83	1.80	0.023	0.394	0.169	0.167	-	1454	2650	122	-
23.01	3825	0.61	35	1.414	5.888	12.98	216.8	31.45	661	1221	0.165	0.118	70.1	230	2924	1.89	1.65	3.54	1.99	0.045	0.775	0.188	0.524	-	1681	3058	88	-
23.01	4243	0.61	35	1.414	5.842	12.88	221.5	32.12	664	1228	0.160	0.115	68.3	224	2773	1.57	1.73	3.30	1.96	0.057	0.990	0.169	0.758	-	1776	3229	84	-
23.01	4675	0.61	35	1.414	6.060	13.36	220.2	31.94	664	1228	0.168	0.121	71.6	235	3041	2.11	1.58	3.69	2.00	0.034	0.596	0.371	0.175	-	1690	3074	109	-
23.01	4912	0.61	35	1.414	5.987	13.20	223.5	32.42	668	1234	0.164	0.118	70.1	230	2904	1.85	1.71	3.56	2.03	0.051	0.902	0.321	0.520	-	1742	3168	85	-
23.01	5086	0.61	35	1.414	5.974	13.17	224.7	32.59	672	1242	0.162	0.117	69.5	228	2870	1.77	1.71	3.48	2.02	0.058	1.002	0.324	0.614	-	1753	3187	82	-
23.01	5426	0.61	35	1.414	6.006	13.24	220.0	31.91	669	1237	0.167	0.120	71.3	234	3017	1.97	1.64	3.61	1.99	0.044	0.763	0.518	0.184	-	1683	3062	90	-
23.01	6604	0.61	35	1.414	5.434	11.98	219.1	31.78	673	1243	0.151	0.109	65.2	214	2507	1.55	1.64	3.19	2.13	0.073	1.282	0.320	0.328	0.555	1904	3460	98	-
23.01	7061	0.61	35	1.414	5.470	12.06	219.7	31.87	672	1242	0.152	0.109	65.2	214	2514	1.62	1.76	3.38	2.24	0.062	1.086	0.332	0.329	0.345	1979	3595	98	-
23.01	9166	0.61	35	1.414	5.538	12.21	218.4	31.67	670	1238	0.155	0.112	66.8	219	2647	1.52	1.76	3.28	2.07	0.056	0.976	0.333	0.348	0.215	1936	3516	96	-
23.01	9856	0.61	35	1.414	5.443	12.00	218.4	31.68	665	1229	0.152	0.109	65.2	214	2530	1.38	1.80	3.18	2.10	0.053	0.921	0.347	0.167	0.339	2046	3713	107	-
23.01	10721	0.61	35	1.414	5.493	12.11	220.2	31.94	660	1220	0.152	0.109	64.9	2.3	2508	1.32	1.69	3.03	2.00	0.070	1.233	0.722	-	0.440	1918	3485	97	-
23.01	10994	0.61	35	1.414	5.493	12.11	215.7	31.28	664	1227	0.156	0.112	66.8	219	2647	1.36	1.70	3.06	1.92	0.064	1.112	0.727	-	0.325	1847	3357	89	-
23.01	11474	0.61	35	1.414	5.942	13.10	220.5	31.98	660	1220	0.165	0.118	70.1	230	2944	1.56	1.70	3.26	1.83	0.050	0.870	0.672	-	0.143	1564	3138	85	-
23.01	12252	0.61	35	1.414	6.010	13.25	222.3	32.24	656	1213	0.165	0.118	70.1	230	2938	1.59	1.71	3.30	1.85	0.050	0.872	0.663	-	0.156	1722	3131	85	-
23.01	13415	0.61	35	1.414	5.715	12.60	217.7	31.57	654	1210	0.160	0.115	68.0	223	2764	1.35	1.73	3.08	1.84	0.056	0.983	0.695	-	0.233	1787	3248	85	-
24.01	176	0.61	35	1.414	5.606	12.36	220.3	31.95	636	1176	0.153	0.110	64.9	213	2493	1.36	1.77	3.13	2.08	0.062	1.090	0.712	-	0.321	1884	3423	93	-
24.01	990	0.61	35	1.414	5.656	12.47	221.2	32.08	629	1164	0.154	0.110	64.6	212	2481	1.37	1.78	3.15	2.04	0.062	1.080	0.704	-	0.315	1673	3403	92	-
25.01	715	0.61	35	0.914	8.274	18.24	224.8	32.61	620	1148	0.223	0.158	91.7	301	5017	4.79	0.64	5.43	1.70	0.012	0.201	0.158	-	-	823	1514	60	-
25.01	2232	0.61	35	0.914	7.217	15.91	222.5	32.27	629	1164	0.196	0.140	81.7	268	3973	3.34	1.15	4.49	1.80	0.022	0.378	0.330	-	-	1144	2091	80	98
25.01	2988	0.61	35	0.914	6.731	14.84	218.9	31.75	612	1134	0.184	0.131	75.9	249	3449	2.42	1.43	3.85	1.75	0.034	0.574	0.520	-	-	1286	2396	71	98
25.01	4231	0.61	35	0.914	6.672	14.71	221.4	32.11	618	1144	0.180	0.129	75.0	246	3349	2.31	1.52	3.83	1.80	0.041	0.703	0.494	-	0.155	1338	2440	65	94
25.01	5662	0.61	35	0.914	6.455	14.23	223.0	32.34	627	1161	0.174	0.125	72.8	239	3173	1.66	1.64	3.30	1.66	0.048	0.835	0.487	-	0.292	1477	2690	68	96
25.01	7160	0.61	35	0.914	6.219	13.71	225.9	32.76	614	1137	0.165	0.117	68.3	224	2795	1.01	1.78	2.79	1.57	0.057	0.976	0.484	-	0.435	1666	3031	76	97
25.01	8547	0.61	35	0.914	6.241	13.76	227.8	33.04	613	1136	0.164	0.117	67.7	222	2762	0.93	1.78	2.71	1.54	0.062	1.059	0.477	-	0.526	1672	3041	76	95
26.01	493	0.61	35	0.914	6.500	14.33	216.7	31.43	621	1150	0.180	0.128	74.7	245	3344	2.07	1.51	3.58	1.69	0.039	0.677	0.622	-	-	1349	2960	68	96
26.01	1881	0.61	35	0.914	7.502	16.54	224.7	32.59	626	1159	0.202	0.144	83.5	274	4178	3.39	1.16	4.55	1.73	0.028	0.482	0.268	-	0.168	1057	1934	54	88
26.01	3156	.61	35	0.914	6.436	14.19	216.4	31.39	623	1154	0.179	0.128	74.4	244	3313	1.83	1.55	3.38	1.62	0.044	0.761	0.706	-	-	1366	2490	63	94
26.01	4659	0.61	35	0.914	6.446	14.21	217.5	31.54	624	1155	0.178	0.127	74.4	244	3295	1.61	1.57	3.38	1.63	0.049	0.838	0.782	-	-	1362	2984	59	94
26.01	6747	0.61	35	0.914	6.269	13.82	224.1	32.51	615	1139	0.167	0.119	69.2	227	2886	1.02	1.75	2.78	1.51	0.055	0.950	0.463	0.432	-	1611	2931	73	-
27.01	3734	0.44	25	0.914	7.956	7.54	220.5	31.98	657	1214	0.225	0.160	94.2	309	2361	4.37	0.66	5.03	1.54	0.012	0.218	0.171	-	-	874	1606	62	88
27.01	5669	0.44	25	0.914	7.149	15.76	220.5	31.98	653	1207	0.200	0.143	84.4	277	1887	2.96	1.14	4.10	1.58	0.022	0.390	0.339	-	-	1168	2134	81	97
27.01	7302	0.44	25	0.914	6.808	15.01	221.7	32.16	631	1168	0.187	0.133	78.0	256	1613	2.26	1.44	3.70	1.63	0.033	0.574	0.519	-	-	1327	2421	76	97
27.01	8394	0.44	25	0.914	6.713	14.80	222.0	32.20	637	1178	0.185	0.132	77.1	253	1589	1.92	1.51	3.43	1.54	0.038	0.664	0.610	-	-	1372	2501	71	96
27.01	9670	0.44	25	0.914	6.527	14.39	218.7	31.72	648	1199	0.184	0.131	77.4	254	1593	1.74	1.53	3.27	1.49	0.044	0.762	0.707	-	-	1382	2520	64	95
27.01	10924	0.44	25	0.914	6.768	14.92	222.5	32.27	646	1194	0.187	0.133	78.3	256	1637	2.11	1.48	3.59	1.58	0.040	0.696	0.496	-	0.148	1338	2441	65	93
27.01	12419	0.44	25	0.914	6.613	14.58	224.1	32.51	644	1191	0.181	0.129	65.9	249	1538	1.70	1.59	3.29	1.54	0.047	0.819	0.478	-	0.287	1432	2610	65	94
27.01	13642	0.44	25	0.914	6.364	14.03	225.7	32.73	647	1196	0.173	0.123	72.8	239	1413	1.31	1.68	3.09	1.53	0.056	0.981	0.981	-	0.444	1569	2857	70	96
27.01	14622	0.44	25	0.914	6.459	14.24	228.8	33.19	641	1186	0.173	0.123	72.5	238	1405	1.02	1.70	2.27	1.39	0.060	1.043	0.472	-	0.516	1573	2864	69	95
29.01	1694	0.79	45	0.914	8.056	17.76	229.0	33.21	632	1169	0.214	0.152	89.0	292	9609	5.02	0.68	5.70	1.93	0.012	0.210	0.166	-	-	875	1607	69	95
29.01	1699	0.79	45	0.914	8.010	17.66	228.1	33.09	634	1173	0.214	0.153	89.3	293	9607	5.18	0.67	5.85	1.98	0.012	0.212	0.167	-	-	868	1595	66	
29.01	3485	0.79	45	0.914	7.135	15.73	228.4	33.13	638	1187	0.189	0.136	79.9	262	7681	3.53	1.21	4.74	2.03	0.022	0.386	0.335	-	-	1241	2266	93	98
29.01	4905	0.79	45	0.914	6.446	14.21	225.5	32.71	634	1173	0.173	0.124	72.5	238	6381	2.33	1.56	3.89	2.00	0.040	0.690	0.634	-	-	1496	2725	80	97
29.01	6780	0.79	45	0.914	6.391	14.09	226.3	32.82	640	1184	0.171	0.123	72.2	237	6335	2.07	1.61	3.68	1.92	0.044	0.775	0.720	-	-	1534	2794	76	97
29.02	4065	0.79	45	0.914	6.405	14.12	220.7	32.01	650	1202	0.176	0.126	74.7	245	6734	2.72	1.45	4.17	2.06	0.036	0.606	0.552	-	-	1431	2608	76	-
29.02	5585	0.79	45	0.914	6.672	14.71	227.7	33.03	642	1187	0.177	0.127	74.7	245	6746	2.64	1.49	4.13	2.02	0.034	0.580	0.527	-	-	1463	2665	83	-
29.02	9615	0.79	45	0.914	6.591	14.53	225.1	32.65	642	1187	0.177	0.127	74.7	245	6730	2.71	1.47	4.18	2.05	0.034	0.596	0.539	-	-	1461	2662	79	97
29.02	11260	0.79	45	0.914	6.219	13.71	224.5	32.56	639	1183	0.167	0.120	70.4	231	6010	1.95	1.65	3.60	1.97	0.043	0.756	0.534	-	0.155	1630	2966	82	96
29.02	12610	0.79	45	0.914	5.715	12.60	220.6	32.00	638	1151	0.156	0.112	65.8	216	5259	1.45	1.76	3.21	2.02	0.055	0.951	0.554	-	0.334	1836	3336	86	97

TABLE I. Test Summary (Cont'd)

Run No.	Point No.	α		L/D	Wa		PT4A		TT4A		M4	Mref	Vref		Swirl	DPSV	DPMOM	DPAUG	CDAUG	F/A	ϕ	ϕ_2	ϕ_3	ϕ_4	TT6		EFFMB	EFFMB
		RAD	DEG		kg/sec	lbm/sec	N/M^2 10^{-3}	PSIA	°C	°F			m/sec	ft/sec	g's	%	%	%							°C	°F	%	Gas Sample
29.02	14165	0.79	45	0.914	5.665	12.49	223.0	32.34	634	1174	0.152	0.109	64.3	211	4998	1.25	1.78	3.03	1.99	0.063	1.088	0.535	-	0.490	1900	3452	89	97
29.02	15324	0.79	45	0.914	5.643	12.44	223.1	32.36	639	1183	0.152	0.109	64.3	211	5008	1.25	1.72	2.97	1.96	0.068	1.187	0.537	-	0.586	1878	3413	90	93
30.01	640	0.61	35	1.373	12.787	28.17	256.7	37.23	656	1213	0.313	0.221	128.3	421	9718	13.40	1.05	14.45	2.36	0.012	0.200	0.161	-	-	909	1668	75	98
30.01	2420	0.61	35	1.373	11.000	24.25	241.6	35.04	648	1198	0.282	0.200	116.1	381	7930	8.92	1.95	10.87	2.16	0.022	0.380	0.332	-	-	1235	2255	91	99
30.01	4150	0.61	35	1.373	10.460	23.06	241.8	35.07	637	1178	0.264	0.188	109.1	358	7026	7.09	2.38	9.47	2.12	0.033	0.565	0.514	-	-	1414	2578	84	97
30.01	5790	0.61	35	1.373	10.187	22.37	240.6	34.90	639	1183	0.258	0.183	106.7	350	6715	6.47	2.52	8.99	2.12	0.039	0.644	0.613	-	-	1501	2734	81	96
30.01	6890	0.61	35	1.373	10.115	22.30	241.7	35.05	640	1184	0.256	0.182	106.1	348	6621	6.40	2.55	8.95	2.14	0.042	0.722	0.671	-	-	1514	2758	77	94
30.01	5461	0.61	35	1.373	9.888	21.80	257.9	37.40	631	1167	0.231	0.165	96.0	315	5439	4.16	3.02	7.18	2.09	0.049	0.835	0.386	0.180	0.218	1913	3476	100	-
30.01	5491	0.61	35	1.373	9.126	20.12	247.2	35.85	628	1163	0.221	0.159	92.4	303	5002	4.06	3.09	7.15	2.256	0.057	0.970	0.375	0.318	0.219	2035	3695	101	-
30.01	5506	0.61	35	1.373	8.831	19.47	238.6	34.61	626	1158	0.222	0.159	92.4	303	5003	3.56	3.11	6.67	2.096	0.059	1.010	0.385	0.338	0.227	2033	3691	100	-
30.02	2475	0.61	35	1.373	9.730	21.45	240.3	34.85	641	1185	0.248	0.176	102.7	337	6246	4.84	2.78	7.62	1.94	0.043	0.748	0.530	-	0.162	1686	3066	89	96
30.02	3775	0.61	35	1.373	8.968	19.77	235.5	34.16	636	1177	0.231	0.165	96.0	315	5464	3.47	3.07	6.54	1.90	0.052	0.893	0.520	-	0.311	1953	3598	100	98
30.02	5110	0.61	35	1.373	8.927	19.68	240.3	35.84	639	1182	0.225	0.161	94.2	309	5225	3.36	3.08	6.44	1.97	0.059	1.013	0.501	-	0.453	2023	3674	100	97
30.02	6689	0.61	35	1.373	8.863	19.54	238.5	34.59	635	1175	0.225	0.161	93.6	307	5180	3.44	3.01	6.45	1.98	0.064	1.104	0.499	-	0.546	1978	3593	96	96
30.02	7830	0.61	35	1.373	8.809	19.42	237.8	34.49	636	1176	0.224	0.160	93.3	306	5154	3.08	3.04	6.12	1.89	0.064	1.107	0.500	-	0.551	2009	3649	99	-
30.02	9490	0.61	35	1.373	9.013	19.87	239.1	34.68	627	1161	0.227	0.162	94.2	309	5234	3.34	3.07	6.41	1.93	0.058	0.997	0.496	-	0.445	1967	3573	96	-
30.02	10855	0.61	35	1.373	10.29	22.68	236.1	34.25	645	1193	0.268	0.190	110.9	364	7270	6.65	2.34	8.99	1.96	0.028	0.484	0.186	0.243	-	1422	2592	95	-
30.02	11165	0.61	35	1.373	10.30	22.71	225.7	32.73	645	1193	0.282	0.200	116.1	381	7997	7.78	2.03	9.81	1.94	0.022	0.366	0.186	0.125	-	1267	2312	98	-
30.02	12495	0.61	35	1.373	11.73	25.87	244.2	35.42	642	1188	0.298	0.211	121.9	400	8779	10.35	1.58	11.9	2.13	0.016	0.277	0.230	-	-	1069	1957	88	-
30.02	13070	0.61	35	1.373	8.582	18.92	231.1	33.52	634	1174	0.224	0.160	93.3	306	5143	3.29	3.07	6.36	1.96	0.062	1.045	0.515	-	0.463	2015	3659	97	-

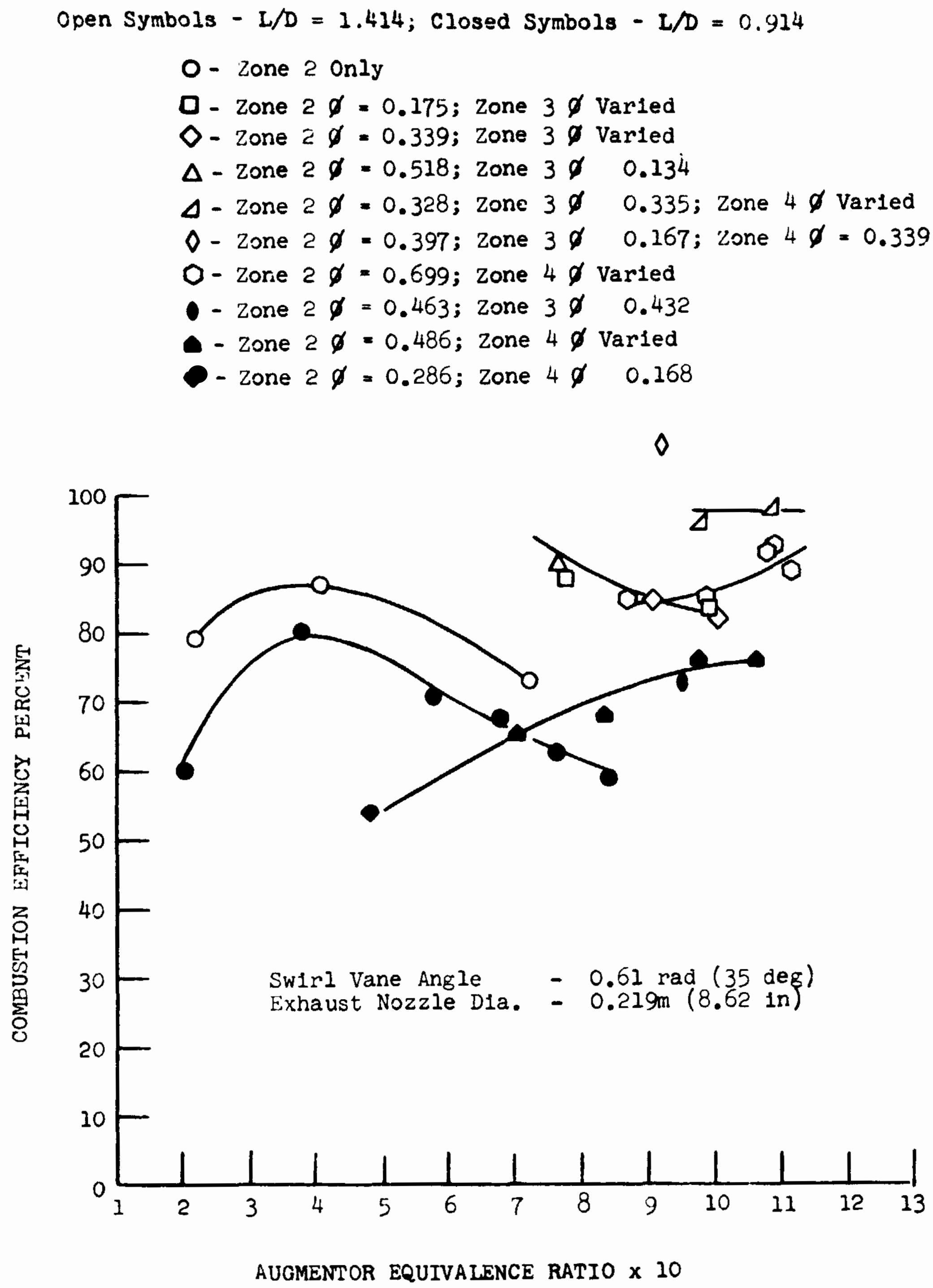

Figure 13. Effect of Augmentor L/D on Combustion Efficiency

smaller L/D the combustion efficiency was reduced by 8 to 10 percent.

Figure 13 also shows, as will subsequent figures, that the zoning of the fuel between the three rig zones had a very large effect on combustion efficiency. As expected, the data show that it was impossible to maintain high efficiencies over the entire operating range with only one zone of fuel injection. In fact, the data show that the highest efficiencies were obtained by gradually adding the fuel from the outside to the center as the fuel loading was increased. Referring to figure 13, as the augmentor equivalence ratio was increased beyond 0.7 the best combustion efficiency was obtained by injecting the fuel through zones 2 and 3. This resulted in nearly a 20 percentage improvement in combustion efficiency at the 0.7 equivalence ratio point when compared to operation with zone 2 only. However, the best combustion efficiency (98 percent at an equivalence ratio of 1.0) was obtained with all three fuel zones operating. In short, the highest combustion efficiencies were obtained as the fuel was more evenly distributed across the duct.

The problem of fuel zoning is complicated by the superposition of a strong swirling flow field on the mainstream flow. When the fuel is injected, it begins to pick up tangential and axial velocity components due to its interaction with the mainstream flow. The tangential velocity component creates a centrifugal force on the fuel mass which tends to drive it toward the outer wall of the duct. The magnitude of this force and its effect on the motion of the fuel mass is continuously changing. This is due, first, to the vaporization of the fuel. As the fuel evaporates, the fuel density decreases, thus, causing a decrease in the magnitude of the centrifugal forces acting on the fuel mass. Also, as the fuel mass moves toward the outer wall, the centrifugal forces acting on it decrease as its radial position increases. These effects, along with the normal turbulent diffusion and mixing of the fuel with the air, complicate the design and location of the sprayring. The scope of this program did not include an investigation of the dispersion of a fuel spray in a strongly swirling flow field. This information would be necessary, however, to minimize development effort for various applications of a swirling flow augmentor.

The effect of increasing swirl intensity on combustion efficiency is shown in figure 14. The data were obtained using the 0.219 meter (8.62 inch) diameter nozzle and 0.44, 0.61 and 0.79 radian (25, 35, and 45 degree) swirl vanes. The augmentor L/D was 0.914. The shorter length was used to more clearly show the effects of increasing swirl intensity. As expected, the combustion efficiency improved as the swirl vane angle and, hence, swirl intensity was increased.

As previously stated, the swirl augmentor combustion efficiency should be insensitive to changes in inlet Mach Number. In figure 15 are plotted data obtained using both exhaust nozzles. The tests were run using the 0.61 radian (35 degree) swirl vanes. The augmentor L/D was 1.4. With the small nozzle the swirl vane inlet Mach Number varies from 0.1 to 0.21 as the equivalence ratio varies from 1.0 to 0.2. With the large nozzle the Mach Number varies from 0.22 to 0.31 over the same range of equivalence ratios.

With zone 2 only and zones 2, 3 and 4 there was very little difference in the results. This is in agreement with the hypothesis that with high through-put velocities there is no effect on efficiency since the flame spreading rate increases in the same proportion as the through put velocity.

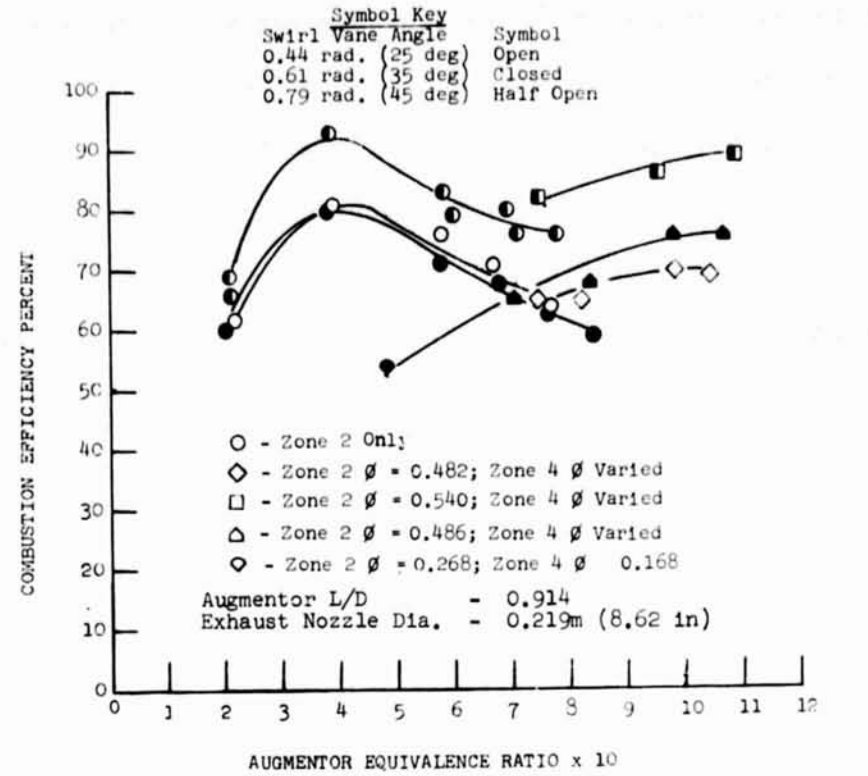

Figure 14. Effect of increasing Swirl intensity on Combustion Efficiency

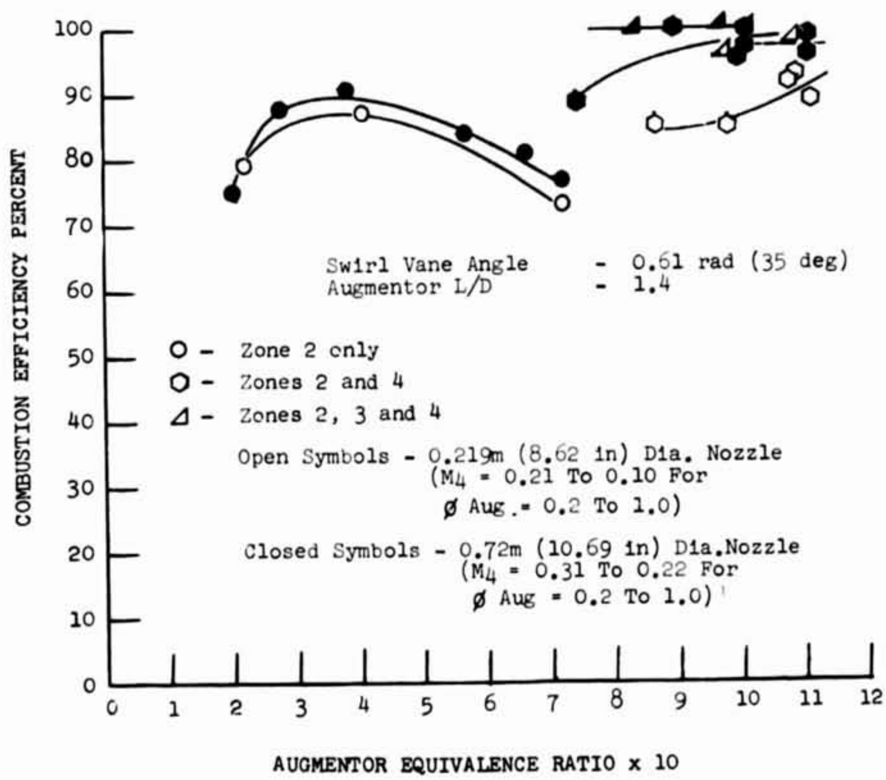

Figure 15. Effect of Mach Number on Combustion Efficiency

With the zone 2 and 4 combinations there was a significant difference in efficiency between the small and large nozzles. This was obviously the result of the type of zoning. Why there is a difference is unknown. However, with the large nozzle, fuel pressure drop is larger and the air velocity over the spraybars in higher. This aids fuel atomization. Also the swirl intensity being larger may have resulted in a different effective zoning.

As mentioned above the combustion efficiency was also determined by sampling the exhaust for unburned hydrocarbon and carbon monoxide. These data are plotted in figures 16 through 19. The data shown in figures 16, 17, and 18 were obtained during the same tests that generated the choked nozzle data of figure 14. The data of figure 19 were taken during the tests that generated the large, choked nozzle data of figure 15. Therefore the corresponding choked nozzle data are also plotted for comparison.

The gas sample calculated efficiency was high (90% or greater) for all values of swirl angle tested and for all equivalence ratios. These data indicate that all of the swirl intensities tested were sufficient to propagate the flame over the entire duct. This is in disagreement with the choked nozzle data.

No substantiated explanation is on hand to account for the large discrepancy in combustion efficiency values as determined by the gas sampling and choked nozzle measurements. Extensive checks of the unburned hydrocarbon and carbon monoxide analyzers before and after each test turned up no problems with the instruments. For most of these tests, especially those at the higher equivalence ratios, the sample temperatures

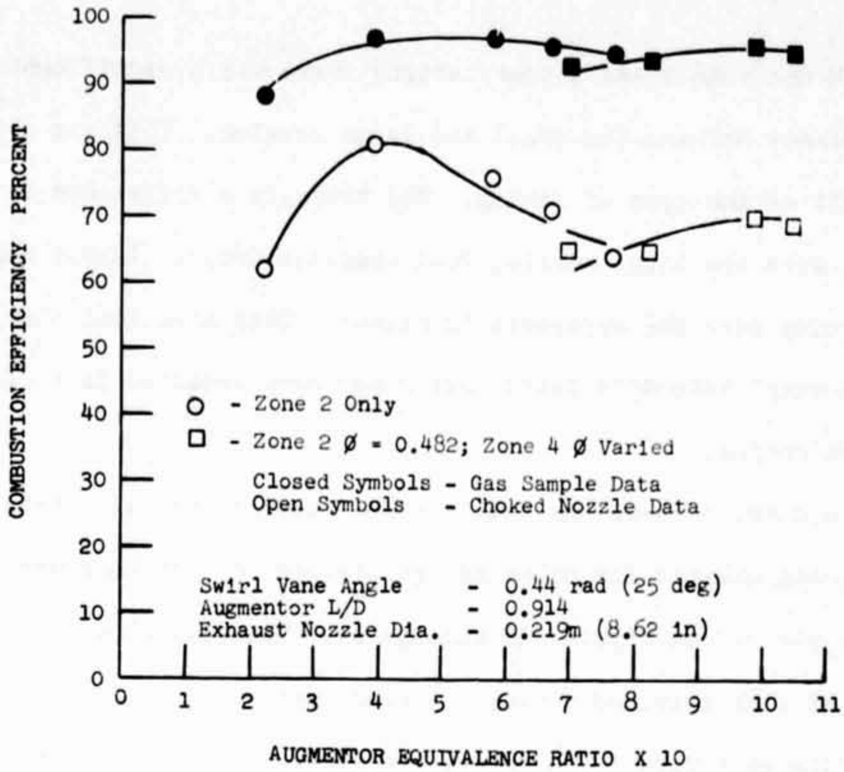

Figure 16. Comparison of Gas Sample and Choked Nozzle Calculated Combustion Efficiencies

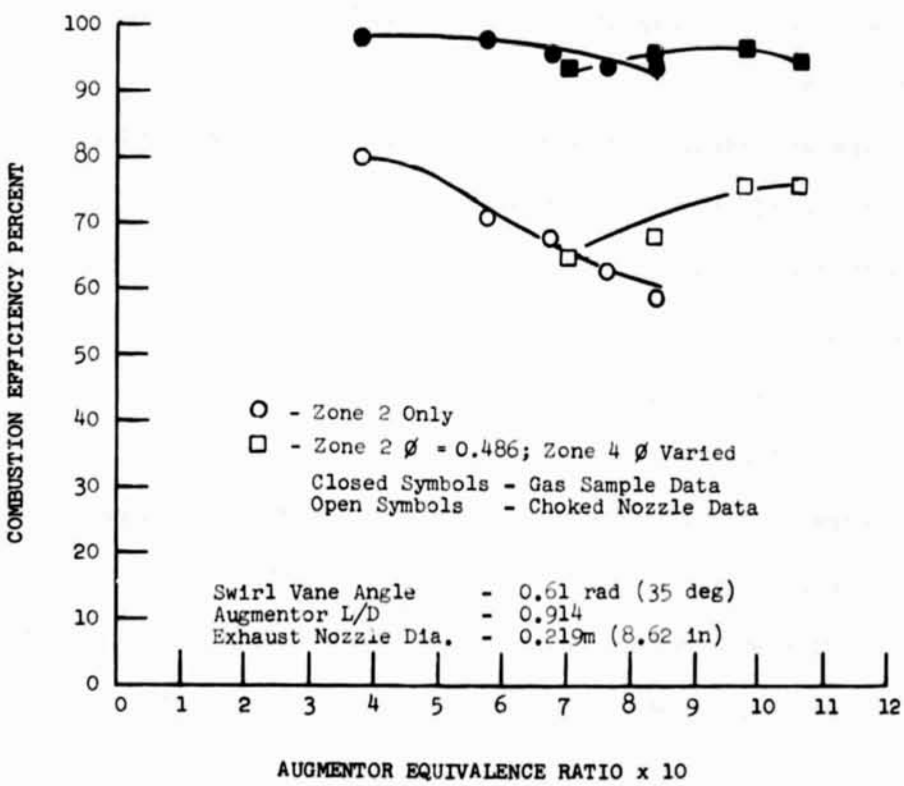

Figure 17. Comparison of Gas Sample and Choked Nozzle Calculated Efficiencies

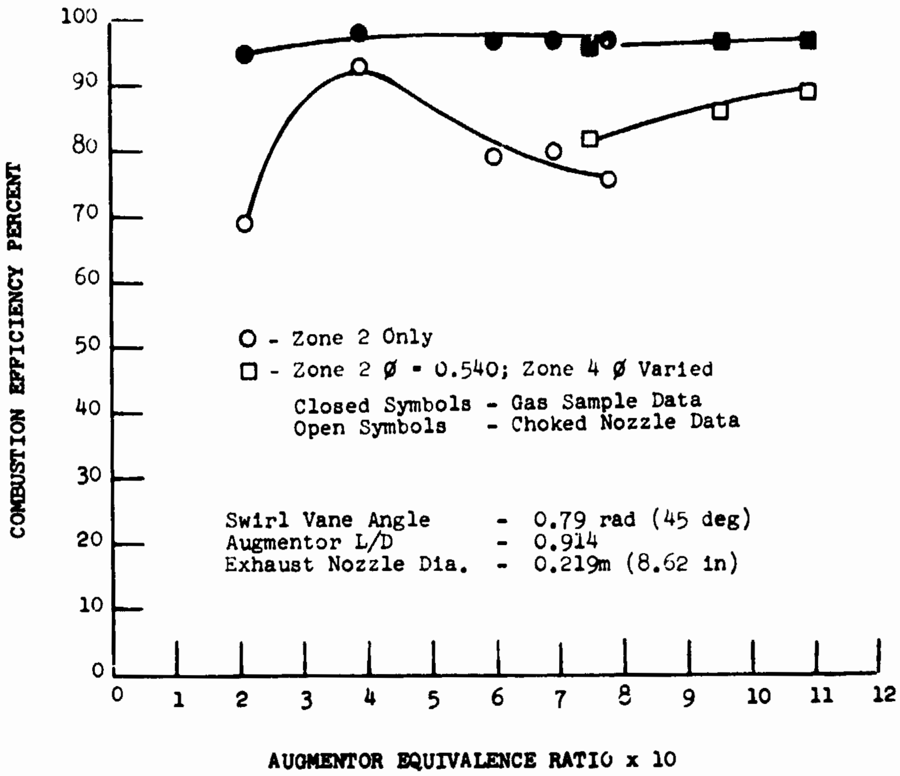

Figure 18. Comparison of Gas Sample and Choked Nozzle Calculated Combustion Efficiencies

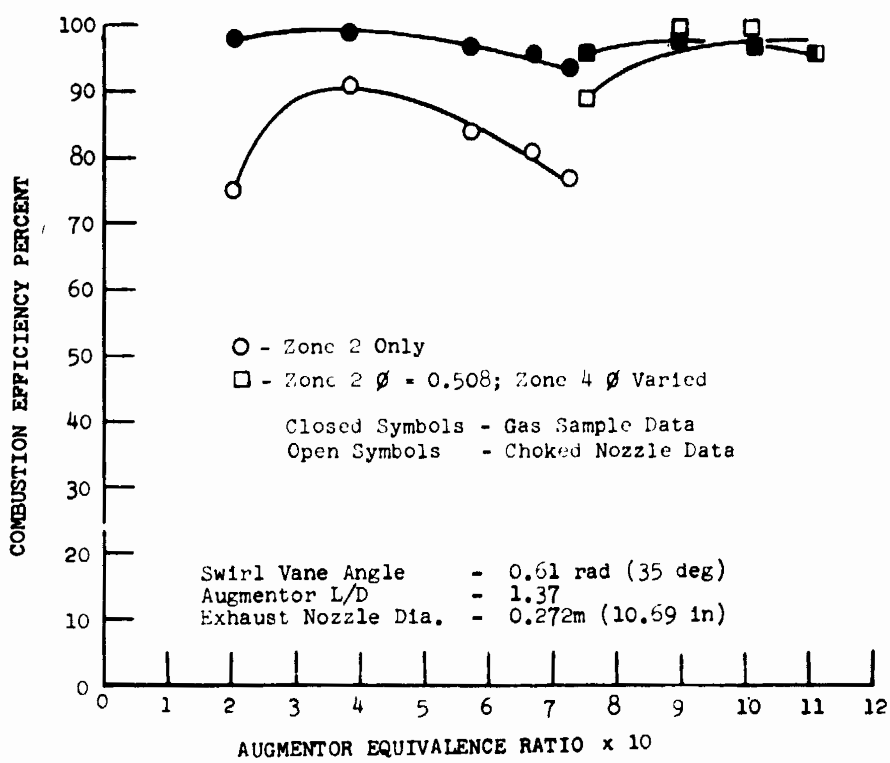

Figure 19. Comparison of Gas Sample and Choked Nozzle Calculated Combustion Efficiencies

were maintained above 149°C (300°F). The samples were obtained with a single point traversing probe located at only one circumferential position. Consequently, there is the possibility that a good representative sample was not obtained.

Another possibility may have been incomplete ignition of the mainstream due to a non-uniform pilot discharge temperature. As mentioned earlier, the pilot was constructed with twenty individual fuel nozzle-swirler combinations equally spaced around the outer circumference of the mainstream. All of the pilot air flow entered the pilot through the swirlers and fuel nozzles only. Consequently, this may have resulted in regions of high and low flow at the pilot zone discharge. With a strongly swirling mainstream flow there is a strong static pressure gradient increasing from the center of the duct to the outer wall. If this gradient is sufficiently strong, there could be a recirculation of cold mainstream gas into the pilot. This would occur if the pilot total pressure in the regions of low pilot flow were not sufficient to overcome the adverse pressure gradient created by the swirling mainstream. This recirculation would result in a very non-uniform pilot discharge tempera-- ture with the possibility that the mainstream would be ignited at discreet locations rather than uniformly around the circumference. As a result, helical tongues of flame would emanate from the pilot and progress toward the center of the rig. The circumferential flame spreading between the individual helixes is governed by turbulent diffusion processes (bouyant forces only act in the radial direction). Conseqently, it would be possible for some of the fuel to pass out of the rig unburned even though the swirl intensity is strong enough to drive the flame to the center of the rig. These unburned exhaust gases would occupy a small portion of the exhaust area, and could be detected only by thorough traversing of the exhaust nozzle.

Typical radial exhaust emission profiles obtained are shown in figures 20, 21 and 22. These data were obtained with the large exhaust nozzle for various combinations of zones 2 and 4 equivalence ratios. These data show that the emission of unburned hydrocarbon as well as the oxides of notrigen were very low. The shapes of the CO emission profiles as more fuel was passed into the zone 4 sprayring may indicate the boundary of the zone 2 and 4 combustion regions.

B. Lean Blowout

An important performance criterion for any augmentor is its lean flammability limit. The only flameholding device in a swirling flow augmentor is the pilot burner. Consequently, the lean flammability limit of the augmentor was taken to be the point where the pilot no longer held flame. This definition was used because as long as the pilot was operating the mainstream flow could be ignited. With the 649°C (1200°F) inlet air temperature, the pilot lean blowout fuel-air ratio was determined to be 0.0007 based on total augmentor airflow. The lean blowout fuel-air ratio based on pilot airflow was 0.015.

C. Total Pressure Loss

Of equal importance with the combustion efficiency is the total pressure loss of the augmentor. In the design of any combustion system there is a tradeoff between combustion efficiency and the total pressure loss necessary to achieve it. The swirling flow augmentor offers the potential of achieving high combustion efficiencies with low pressure losses since flameholders are not needed. In this type of augmentor,

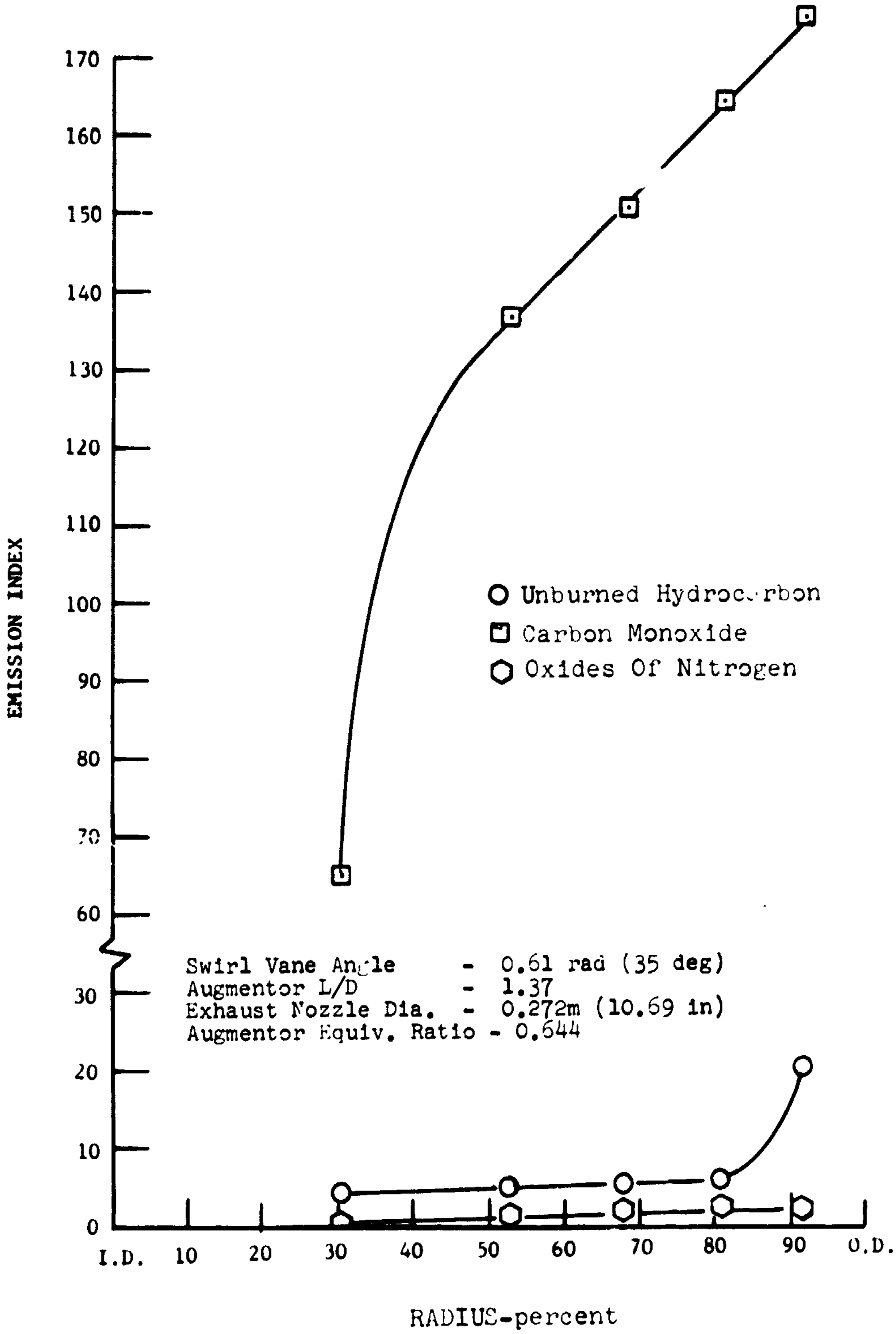

Figure 20. **Exhaust Radial Emission Profiles using Zone 2 only**

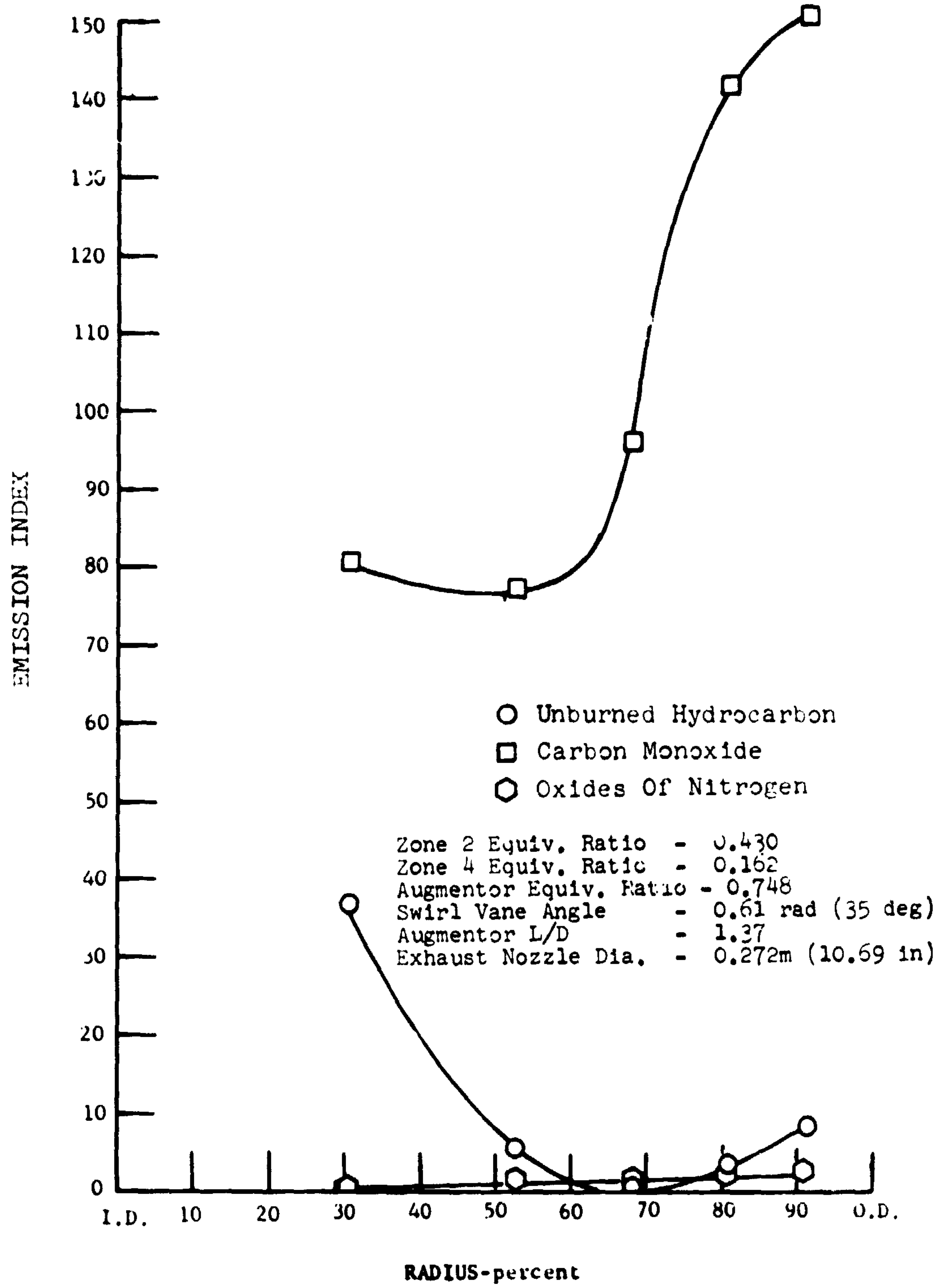

Figure 21. Exhaust Radial Emission Profiles using Zone 2 and Zone 4

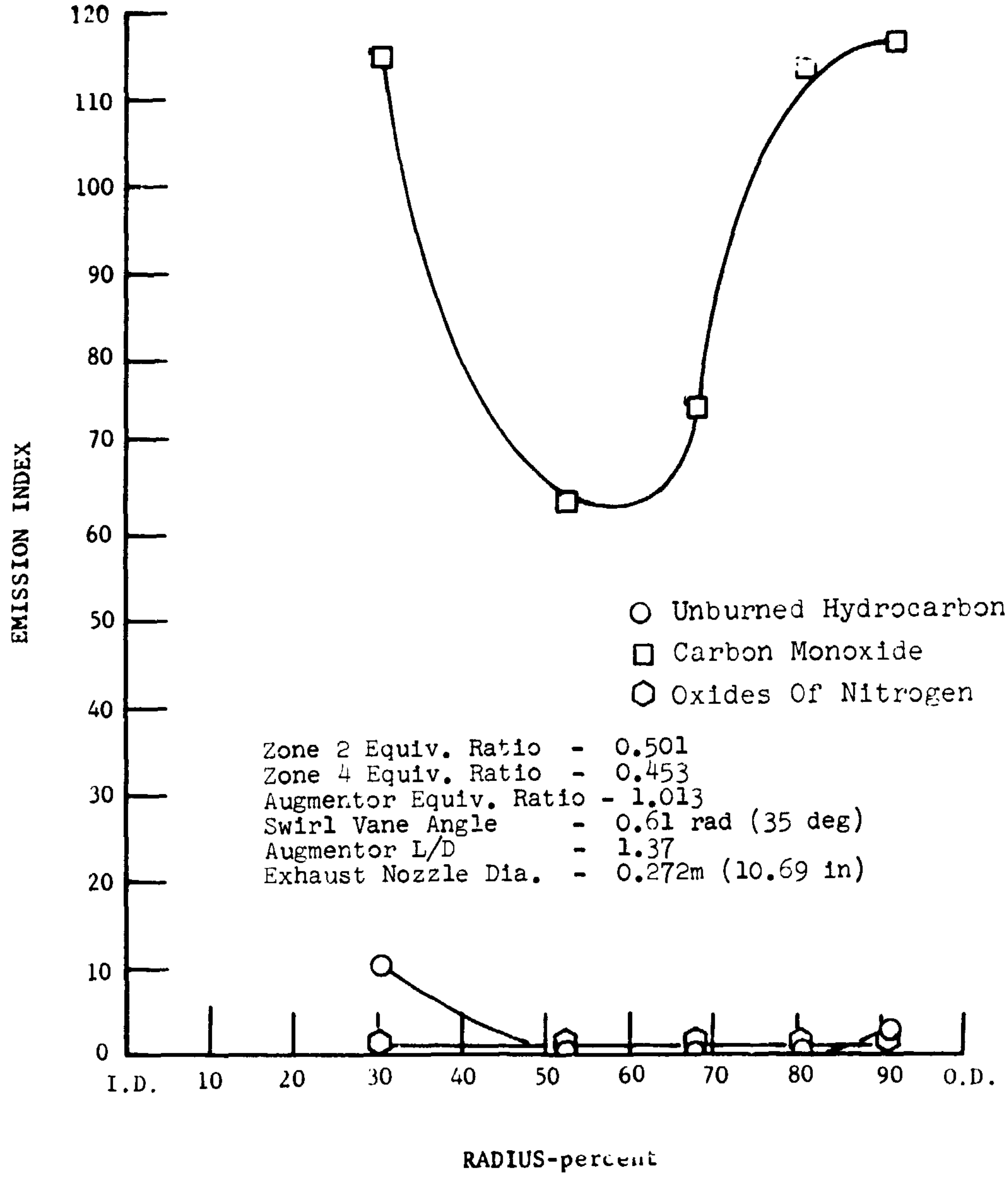

Figure 22. **Exhaust Radial Emission Profiles using Zone 2 and Zone 4**

cold flow total pressure losses result primarily from the creation of the strongly swirling flow field. Of course, when in operation there are always the inescapable losses due to heat addition. Current experience in the design of turbines indicate that the level of turning used in the program can be obtained with losses on the order of 2 or 3 percent.

The augmentor pressure losses plotted in figure 23 are in the form of a drag coefficient which is:

CDAUG = DPAUG/Q4

where

CDAUG = augmentor drag coefficient

DPAUG = augmentor total pressure loss

Q4 = dynamic head of the inlet flow

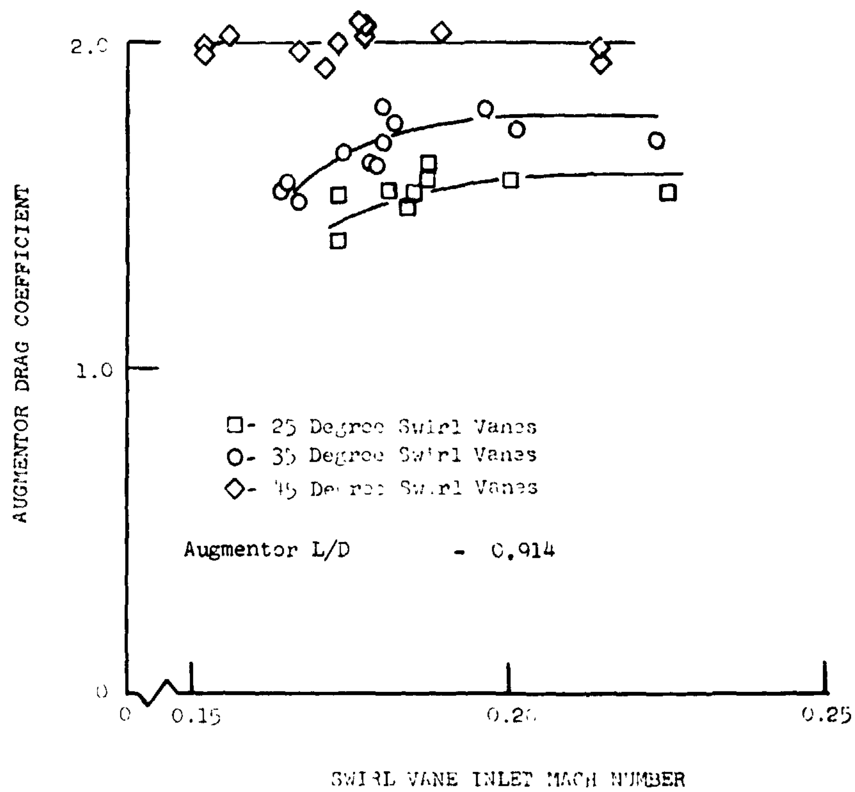

Figure 23. Effect of Mach Number and Swirl Intensity of Augmentor Drag Coefficient

Figure 23 shows the relative effect of increasing swirl intensity on the augmentor drag coefficient. The augmentor was equipped with the smaller nozzle and its L/D was 0.914. As expected, the highest losses were obtained with the 0.79 radian (45 degree) vanes and the lowest with the 0.44 radian (25 degree) vanes.

An obvious result of the data in figure 23 is that the losses were high. This result could negate any benefit due to the improvement in combustion efficiency. With this in mind, a review of the data as well as the rig and swirl vane design was undertaken to determine the possible causes of the high measured pressure losses.

One source of the high measured losses was found to be in the measurement of the inlet total pressure. Figure 24 shows the location of the two total pressure probes used to measure the inlet total pressure. Both sensors were located midway between the turbine simulator vanes. In this location they sensed the maximum total pressure. If more sensors had been used and located so as to obtain a better average pressure the inlet average pressure would have been lower. This would result in lower measured vane losses. Following completion of this contract, additional tests were conducted under an Independent Research and Development Program with the turbine simulator vanes removed. The results of these tests are shown in figure 25. The data shown were obtained using the large nozzle both with and without the turbine simulator vanes. The data points shown are the vane cold flow losses. They were determined by subtracting out the losses due to heating from the measured overall total pressure losses.

The large scatter in the data obtained without the turbine simulator vanes is due to the fact that data were hand recorded. The normal

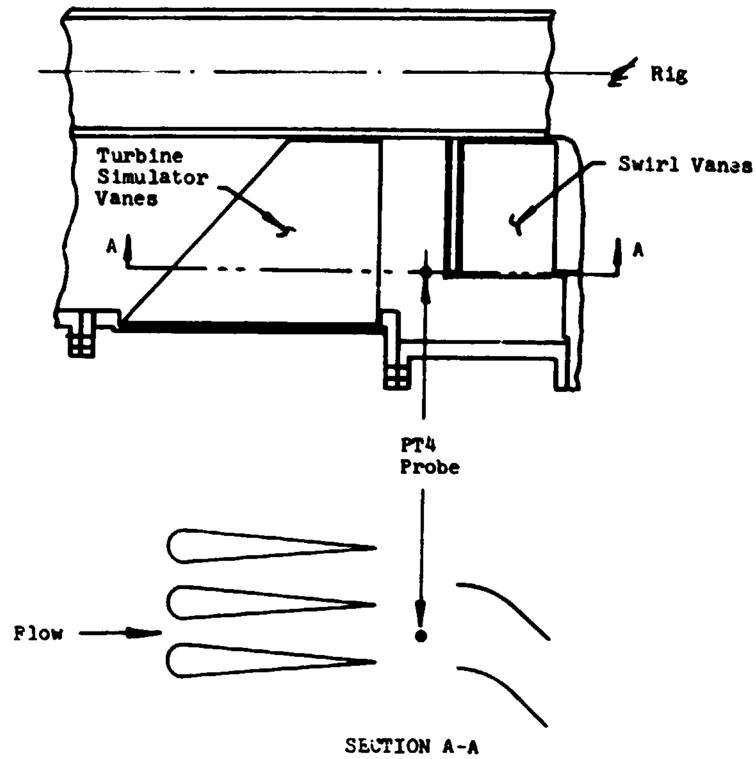

Figure 24. Location of Inlet total Pressure Probes

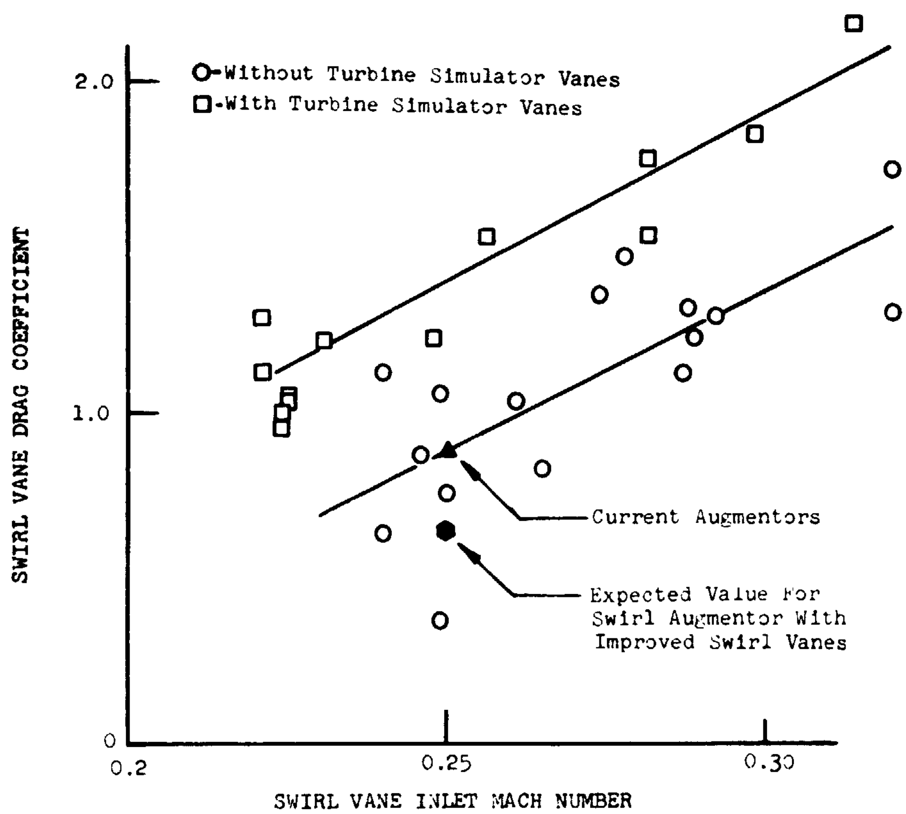

Figure 25. Comparison of Swirl Vane Drag Coefficients with and without the Turbine Simulator Vanes Installed

procedure was to use a high speed data recording system which recorded each channel ten times per second. The data were then averaged over five second intervals. In this way a good average value of each parameter was obtained. By hand recording the data each data channel was recorded only one time. Consequently, a good average value for each data channel was not obtained. Also, the recording time extended over approximately ten minutes, thereby, increasing the possibility for changes in the test conditions due to air and fuel supply fluctuations. However, the data do show that removal of the turbine simulator vanes did cause a significant drop in the measured swirl vane pressure drop. Figure 25 shows a typical cold flow drag coefficient of current high performance augmentors. As can be seen the true drag coefficient of the experimental swirl augmentor (the drag coefficient obtained with the turbine simulator vanes removed) is equal to that of current augmentors at the same conditions.

As mentioned earlier, the swirl vanes were simple curved sheet metal vanes. No attempt was made to contour the vanes to minimize vane profile losses. With well contoured vanes, cold flow drag coefficients on the order of those shown on figure 25 may be possible. This represents a 28 percent reduction in the cold flow pressure loss.

D. Effect of Swirl on Nozzle Thrust Coefficient

Of immediate concern when considering the use of swirling flow in augmentors is what effect does swirl have on the performance of the exhaust nozzle. Data reported in the literature (ref. 4) show that swirl reduces the discharge coefficient. However, of more practical concern is the effect of swirl on the thrust coefficient of the nozzle. Because of its relevance to the program discussed herein, the result of an Independent Research and Development Program which was conducted to obtain this information is presented.

Figure 26 is a plot of nozzle thrust coefficient against the median swirl angle at the nozzle throat. The data were obtained using convergent nozzles only. The throat median swirl angle is defined as the swirl angle at the midspan radius. As can be seen, for throat midspan swirl angles less than 0.26 radians (15 deg) there is no effect on the nozzle thrust coefficient. Above this angle the thrust coefficient begins to fall rapidly.

In figures 27 and 28 are plotted the nozzle throat swirl angle profiles obtained using the 0.219 meter (8.62 inch) diameter nozzle. The data of figure 27 are cold flow data. The data of figure 28 were obtained at an augmentor equivalence ratio of 0.75. The midspan was approximately 0.055 meters (2.15 inches). Note that as the augmentor equivalence ratio was increased the midspan swirl angle decreased from approximately 0.34 radians to 0.26 radians (19.5 to 15 degrees). This is to be expected since increasing the combustor outlet temperature, with a fixed area nozzle, decreases the combustor inlet velocity, both axial and tangential, so the tangential velocity at the exhaust nozzle is reduced and because of the higher outlet temperature the axial velocity at the nozzle is increased. With a variable area nozzle the midspan swirl angle would still decrease because the increase in gas temperature raises the axial velocity.

Therefore, in a practical swirl augmentor system it may be desirable to adjust the swirl vane angle in order to maintain the thrust coefficient at the non-swirl value. However, this should not reduce performance since less swirl is needed to maintain high combustion efficiency as the equivalence ratio is lowered. An additional benefit of adjustable swirl vanes

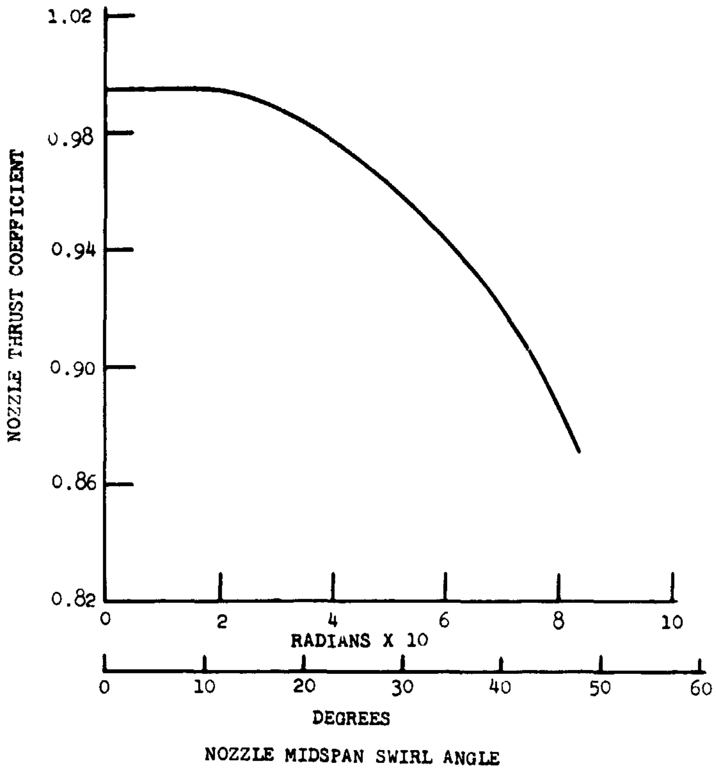

Figure 26. Effect of nozzle midspan swirl angle on the nozzle thrust coefficient

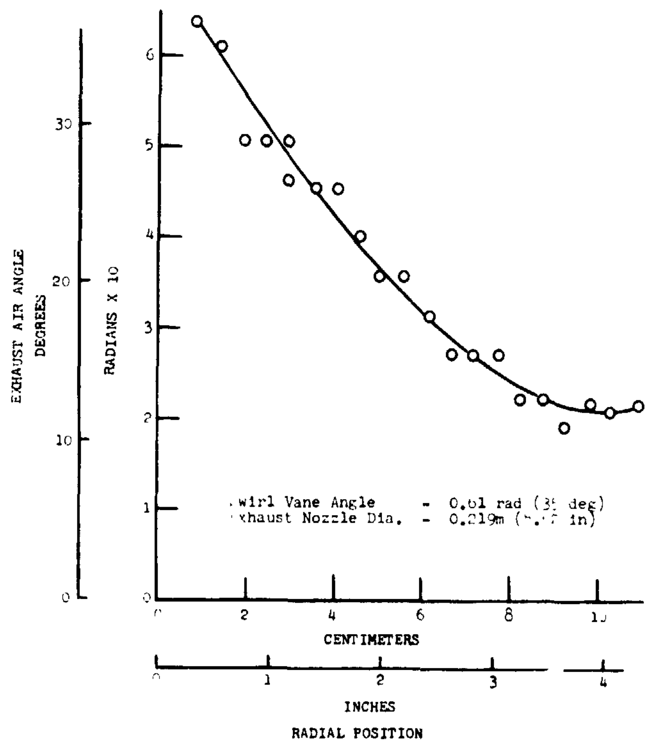

Figure 27. **Measured Exhaust Air Angle Profile Obtained during Cold Flow**

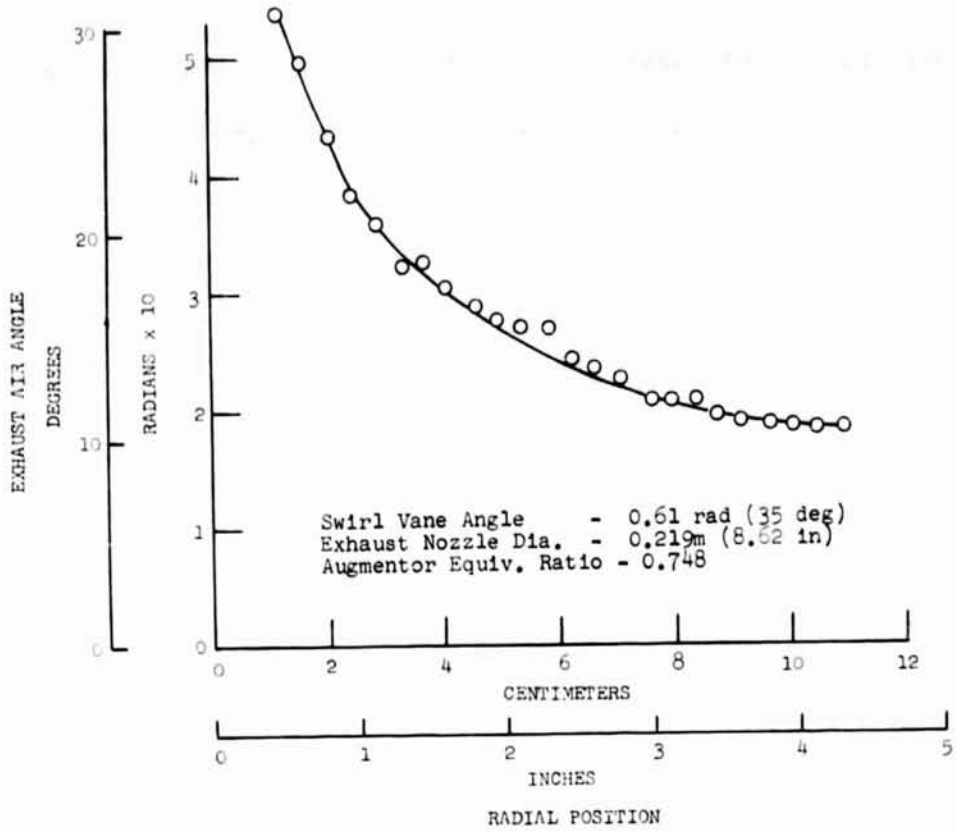

Figure 28. Measured Exhaust Air Angle Profile

would be that non-burning pressure losses could be made very low by setting the vanes to provide axial flow. Since there are no flameholders in the stream the non-burning losses should be well below those of conventional systems.

E. Combustion Instabilities

In the design and development of an augmentor, combustion instabilities can be a problem. The swirling flow augmentor was no different. During contractor funded tests prior to the start of the program combustion instabilities (screech) occurred with frequencies between 500 and 1000 Hz, depending on the inlet temperature. An acoustic liner, mentioned earlier, was designed and proved very effective in eliminating these instabilities. During the course of contract testing instabilities in the 90 to 100 Hz frequency range (commonly referred to as rumble) occurred.

It was found that these instabilities could be circumvented by proper fuel zoning. By properly zoning the fuel the augmentor was operated over the entire range of equivalence ratios without the occurrence of rumble.

SUMMARY OF RESULTS

A test program was conducted with an augmentor which employed swirling flow as a means of promoting rapid flame propagation. The tests were conducted at 2 atmospheres pressure and 649°C (1200°F) inlet air temperature. Significant test results are as follows:

1. At the full power test condition (equivalence ratio of 1.0) the swirl augmentor demonstrated a combustion efficiency of 100%.
2. The measured total pressure losses were typical of current high performance conventional augmentors. Current experience indicates that with well designed turning vanes the cold pressure losses can be reduced by 28 percent.
3. The best performance in terms of combustion efficiency, pressur loss and augmentor length was obtained with an augmentor L/D of 1.4 and a swirl vane angle of 0.61 radians (35 degrees).
4. Proper zoning of the fuel flow to the augmentor was found to be essential to maintain high combustion efficiency. The best results were obtained by gradually injecting the fuel from the outside to the center as the fuel loading was increased.
5. The augmentor lean blow-out was 0.0007 based on total augmentor airflow at the 1200°F inlet temperature test condition. The lean blow-out point is strictly dependent on the flammability limit of the pilot burner.
6. Combustion instabilities, both screech and rumble, did occur at certain operating conditions during the test program. However,

screech in the frequency range between 500 and 1000 Hz was suppressed with a conventional type acoustic liner. Rumble in the frequency range between 90 and 100 Hz was avoided by proper distribution of fuel to the three fuel sprayrings.

APPENDIX A
SWIRL AUGMENTOR PERFORMANCE CALCULATIONS

An engineering type formulation of the data reduction deck used to process the swirl augmentor data is presented. The formulation is not intended to present the detailed logic performed by the performance deck. Instead, only the main concepts and equations used to determine the various performance parameters are given.

The gas is assumed to obey the perfect gas law and the flow processes are described by the one dimensional, isentropic relations for compressible fluid flow. A list of symbols is presented in Appendix B.

1. Airflow Metering Orifice Temperature

This is the airflow total temperature at the primary airflow orifice. The temperature is the arithmetic average of two temperatures measured with chromel/alumel thermocouples, or

$$TORF = (TORF1 + TORF2)/2 \qquad (1)$$

2. Airflow Metering Orifice Pressure

The airflow metering orifice upstream pressure (PORF1) is measured with one flange static pressure tap.

3. Airflow Metering Orifice Delta P

The airflow metering orifice delta P (DPORF) is measured with a differential pressure transducer connected across the orifice upstream and downstream flange taps.

4. Airflow Metering Orifice Diameter

The orifice diameter is input to the performance deck. The primary orifice diameter is 0.184 meter (7.250 in.).

5. Rig Total Airflow

This is the total rig dry airflow as measured with the 0.184-meter (7.25-in.) diameter orifice. The orifice measures total massflow (dry airflow plus water vapor) by the following equation:

$$\text{MASSFLOW} = 31.2713 \left[1.0 - 0.3584 \ (\text{DPORF}/\text{PORF1})\right] * \sqrt{(\text{DPORF}) \ (\text{PORF1})/\text{TORF}} * \left[0.9983478 + 0.2065217 \times 10^{-4} \ \text{TORF}\right] \quad (2)$$

The last terms in parenthesis correct the massflow for changes in orifice area due to thermal expansion.

The dry airflow rate is calculated by subtracting the mass of water vapor present in the inlet massflow. This procedure is not as simple as it sounds because the presence of water vapor in the mixture changes the gas properties from those for dry air. Since the coefficients in equation (2) are based on dry air, the massflow calculated by it will be in error. This is due to the changes in gas properties brought about by the water vapor in the mixture. The procedure used to calculate the dry airflow rate is as follows. First the gas properties for several mixtures of dry air and water vapor are determined. The gas constant for each mixture is given by:

$$R_m = \frac{R_a W_a + R_w W_w}{W_a + W_s} = \left(R_a + \frac{R_w W_w}{W_a}\right) \Big/ \left(1 + \frac{W_w}{W_a}\right) \quad (3)$$

Where W_w is the mass of water vapor and W_a is the dry airflow rate. Since W_w/W_a is the specific humidity, the gas constant for the mixture is:

$$R_m = (R_a + R_w \ \text{HUM}) \ / \ (1 + \text{HUM}) \quad (4)$$

The specific humidity is calculated from psychrometric charts for measured values of wet and dry bulb temperatures.

The specific heat ratio for the mixture of dry air and water is given by:

$$\gamma_m = C_{pm}/(C_{pm} - R_m) \quad (5)$$

The specific heat for the mixture, C_{pm}, is given by:

$$C_{pm} = (C_{pa} + C_{pw} \ \text{HUM}) \ / \ (1 + \text{HUM}) \quad (6)$$

From the above equations, the gas constant and specific heat ratio for several dry air and water vapor mixtures (specific humidities) were calculated. Using the following equation, the ratio of airflow computed using wet properties to that using dry properties, C_f, was determined for the various values of specific humidity.

$$C_f = \left[\frac{\left[1 + \left(\frac{A_2}{A_1}\right)^2 \left(\frac{P_2}{P_1}\right)^{2/\gamma a}\right] \left[\frac{\gamma_m}{R_m\,(\gamma_m - 1)} \left(\frac{P_1}{P_2}\right)^{\frac{\gamma_m - 1}{\gamma_m}} \left(\left(\frac{P_1}{P_2}\right)^{\frac{\gamma_m - 1}{\gamma_m}} - 1\right)\right]}{\left[1 + \left(\frac{A_2}{A_1}\right)^2 \left(\frac{P_2}{P_1}\right)^{2/\gamma m}\right] \left[\frac{\gamma_a}{R_a\,(\gamma_a - 1)} \left(\frac{P_1}{P_2}\right)^{\frac{\gamma_a - 1}{\gamma_a}} \left(\left(\frac{P_1}{P_2}\right)^{\frac{\gamma_a - 1}{\gamma_a}} - 1\right)\right]} \right]^{1/2} \qquad (7)$$

Where P_2 is the orifice throat static pressure and P_1 is the orifice upstream pressure. The subscript "a" refers to dry air and the subscript "m" to the dry air and water vapor mixture. These calculations yielded a functional relation between the mass ratio, C_f, and specific humidity which was approximated with a linear curve fit with the following result:

$$C_f = \frac{\text{Computed Flow Using Wet Properties}}{\text{Computed Flow Using Dry Properties}} \qquad (8)$$

$$C_f = 1 - 0.3\ \text{HUM}$$

The calculated massflow is that calculated by equation (2). The dry airflow is then given by:

$$W_a = \text{Calculated Massflow}\ (1 - 0.3\ \text{HUM})\ /\ (1 + \text{HUM}) \qquad (9)$$

6. Secondary Orifice Upstream Pressure

This orifice is used only as a back-up to the 7.25-in. orifice in case difficulty with any of the measured parameters should render that orifice useless. It has a diameter of 0.173 meters (6.83 in.). As long as good data are obtained with the primary orifice, the airflow as measured with this orifice is not used in subsequent performance calculations. The orifice upstream pressure (BA FP1) is measured with a single static pressure flange tap.

7. Secondary Orifice Delta Pressure

This pressure (BAFDP) is measured with a single differential pressure transducer connected across the upstream and downstream static pressure taps.

8. Secondary Orifice Temperature

This temperature is the arithmetic average of two chromel-alumel thermocouples or

$$BAFTTA = (BAFTT1 + BAFTT2) / 2 \qquad (10)$$

9. Secondary Orifice Airflow

The total orifice massflow is calculated with the following equation:

$$MASSFLOW = 26.80\,[1.0 - 0.327\,(BAFDP/BAFP1)] * \sqrt{BAFDP(BAFP1)/BAFTTA} * [0.9983478 + 0.2065217 \times 10^{-1}\,BAFTTA] \qquad (11)$$

This massflow is not corrected for water vapor unless this orifice becomes the primary airflow metering device. If it is the primary orifice the humidity corrections are the same as outlined in paragraph 5.

10. Pilot Airflow

To calculate the pilot zone airflow the pressure drop across the pilot must first be determined. This is done as follows. The pilot downstream pressure is given by:

$$PSP = PS5A\,(1 + DPMOM/100) \qquad (12)$$

Where PS5A is the combustion chamber static pressure, see paragraph 37, and DPMOM is the momentum pressure loss in percent, see paragraph 18. The pilot system pressure ratio is:

$$PR = PSP/PT4A \qquad (13)$$

Where PT4A is the augmentor inlet total pressure, see paragraph 29. Using this pressure ratio the Mach number across the pilot is:

$$M_{pz} = \sqrt{\left(\frac{2}{GAM4-1}\right)\left[\left(\frac{1}{PR}\right)^{\frac{GAM4-1}{GAM4}} - 1\right]} \qquad (14)$$

Where the specific heat ratio, GAM4, is calculated as outlined in paragraph 28. Knowing the Mach number, the pilot airflow is given by:

$$W_{pz} = PT4A\,(A_p)\,(M_{pz})\sqrt{\frac{GAM4(G)}{R_4(TT4A)}\left[\frac{1}{\left(1+\frac{GAM4-1}{2}M_{pz}^{2}\right)^{\frac{GAM4-1}{GAM4+1}}}\right]} \qquad (15)$$

The rig inlet total temperature, TT4A, is calculated in paragraph 30. The pilot effective area, A_p, was determined experimentally to be 24.47 cm^2 (7932 in.^{2}).

11. Pilot Zone Fuel Delta P

The pilot zone fuel pressure drop is simply:

$$DPFPZ = PFPZ - PT4A \qquad (16)$$

12. Pilot Zone Fuel Flow

The pilot fuel flow, WFPZ, is measured with a turbine type flowmeter.

13. Pilot Zone Local Fuel/Air Ratio

The pilot fuel/air ratio is:

$$FAPZ = WFPZ/3600\ WPZ \qquad (17)$$

14. Preheater Inlet Temperature

This temperature is the arithmetic average of two chromel-alumel thermocouples located immediately upstream of the preheater inlet.

$$TT3A = (TT31 + TT32)/2 \qquad (18)$$

15. Specific Humidity

The specific humidity is determined from measured values of wet and dry bulb temperatures using a curve fit of the psychometric charts.

16. Cooling Water Flow

The cooling water flowrate is given by:

$$WCW = 0.5955\sqrt{DP_w\ \rho_w} \qquad (19)$$

Where

DP_w = Pressure drop across a 0.031 meter (1.225 in.) diameter orifice meter

ρ_w = Water density

The water density is calculated as a function of temperature by:

$$\rho_w = 62.41344 + 0.003019152\ (TWORF) - 0.00007294372\ (TWORF)^2 \quad (20)$$

17. Heat Loss to Cooling Water

The heat rejected to the water is calculated by:

$$Q_{loss} = 1.009\ WCW\ (TWORF - TWIN) \quad (21)$$

18. Zone 2, 3 or 4 Fuel Delta P

The fuel pressure drop for zones 2, 3 and 4 is simply

$$DPFZ\ 2,\ 3\ or\ 4 = PFZ\ 2,\ 3\ or\ 4 - PT4A \quad (22)$$

19. Zone 2, 3 or 4 Fuel Flow

The fuel zone fuel flows are measured with turbine type flow meters.

20. Zone 2, 3 or 4 Fuel-to-Air Ratio

The fuel-to-air ratio for zones 2, 3 or 4 is simply:

$$FA2,\ 3,\ or\ 4 = WFZ2,\ 3\ or\ 4/3600\ W_a \quad (23)$$

21. Zone 2, 3 or 4 Equivalence Ratio

The zone 2, 3 or 4 equivalence ratio is given by:

$$\Phi\ 2,\ 3\ or\ 4 = FA\ 2,\ 3\ or\ 4/\ (0.0681 - FAPH) \quad (24)$$

Where FAPH is the preheater fuel-to-air ratio calculated in paragraph 50. The 0.0681 term in the denominator is the stoichometric fuel/air ratio for JP-5 type kerosine.

22. Augmentor Fuel Flow

The augmentor fuel flow is simply the sum of the pilot and zones 2, 3 and 4 fuel flows or:

$$WFT = WFPZ + WF2 + WF3 + WF4 \quad (25)$$

23. Augmentor Fuel-to-Air Ratio

The augmentor fuel-to-air ratio is given by:

$$FAO = WFT/3600\ W_a \tag{26}$$

24. Augmentor Equivalence Ratio

The augmentor equivalence ratio is given by:

$$\Phi = FAO/\ (0.0681 - FAPH) \tag{27}$$

25. Pilot Type

This heading refers to the type swirler used in the pilot zone. This is an input value denoted with either a 1 or 2. The initial rig design provided for two pilot swirler designs. In one swirler design the airflow entered in an axial direction; hence, the swirler is referred to as a coaxial swirler. In the second design the airflow entered the swirler in a radial direction, hence, it is referred to as a radial inflow swirler. An input value of 1 refers to the coaxial swirler and a value of 2 to the radial inflow swirler. All tests under this contract were run with the coaxial swirler.

26. Nominal Swirl Vane Angle

This heading is also an input value and refers to the nominal turning angle of the swirl vane set in use. There are three vane sets having nominal swirl angles of 0.44, 0.61 and 0.79 radians (25, 35 and 45 deg).

27. Combustion Zone Length

The effective combustion length is calculated by adding to the combustion chamber length an equivalent duct of the same diameter whose volume is equal to the volume of the exhaust nozzle. This is given by:

$$L = \text{Combustion Chamber Length} + \text{Exhaust Nozzle Volume}/A_5 \tag{28}$$

The combustion chamber length is taken as the length from the plane of the zone 2, 3 and 4 sprayrings to the nozzle inlet. A_5 is the flow area of the combustion chamber which is 0.114 m^2 (176.63 $in.^2$).

28. Rig Inlet Static Pressure

The rig inlet static pressure is calculated using the relations for one-dimensional isentropic flow of a perfect gas. From the measured values of temperature (TT4A, see paragraph 30), pressure (PT4A, see paragraph 29), dry airflow, specific humidity, and preheater fuel flow the Mach number is calculated by iterating on the following equation:

$$M_{4.5} = \frac{W_a\,(1 + HUM + FAPH)}{PT4A\,(A_{4.5})} \sqrt{\frac{R_4(TT4A)}{GAM4(G)} \left[1 + \frac{GAM4-1}{2} M_{4.5}^2\right]^{\frac{GAM4-1}{GAM4-1}}} \tag{29}$$

The iteration is carried to the accuracy limit of the computer which is to seven significant figures. The gas constant (R_4) for the mixture of air, water vapor, and preheater fuel was determined in the following manner:

$$R_4 = \frac{R'\,(W_a + WFPH) + R_w\,W_w}{W_a + WFPH + W_w} \tag{30}$$

R' is a theoretical gas constant obtained from a propellant performance program for the products of combustion from the stand preheater at the preheater operating conditions.

The specific heat ratio (GAM4) for the mixture of air, water, and fuel was determined as follows:

$$GAM4 = C_{p4}/(C_{p4} - R_4) \tag{31}$$

This required calculation of the specific heat for the mixture:

$$C_{p4} = \frac{C_p'\,(W_a + WFPH) + C_{pw}\,(W_w)}{W_a + WFPH + W_w} \tag{32}$$

C_p' is a theoretical specific heat obtained from the propellant performance program for the products of combustion from the stand preheater at the preheater operating conditions. C_{pw} is the specific heat for water vapor at the preheater exhaust temperature. The area, $A_{4.5}$, is the annular area between the 0.432 meter (17 in.) inner diameter of the pilot case and the 0.102 meter (4 in.) center body, or, 0.138m^2 (214.4 in.^{2}). Knowing the Mach number the rig inlet static pressure is given by:

$$PS4.5 = PT4A / \left[1 + \frac{GAM4-1}{2} M_{4.5}^{2} \right]^{\frac{GAM4}{GAM4-1}} \tag{33}$$

29. Rig Inlet Total Pressure

The rig inlet total pressure is an arithmetic average of two pressures measured with Kiel type total pressure probes. Therefore,

$$PT4A = (PZP1 + PZP2) / 2 \tag{34}$$

30. Rig Inlet Total Temperature

The rig inlet total temperature is taken as the ideal preheater outlet temperature, TT4IDEAL. TT4IDEAL is determined from an enthalpy balance across the preheater. Therefore:

$$H_4 = H_{win} + H_a + H_f = H_{win} + H_c \tag{35}$$

Where

H_{win} = Enthalpy of the water vapor in the inlet flow

H_a Enthalpy of inlet air

H_f Enthalpy of fuel plus lower heating value of 18,370 Btu/lb_m

H_c Enthalpy of combustion products

Note the enthalpy of the water was considered constant. This arises from the assumption that the water does not enter into combustion process but is ideally mixed with the combustion products at the final mixture temperature. All the above enthalpies are total enthalpies and include any kinetic energy associated with each component. Therefore,

$$W_t \, C_{p4} \, TT4IDEAL = W_w \, C_{pw} \, TTWIN + W_c \, C_p' \, TTC$$

rearranging (36)

$$TT4IDEAL = TTC \left(\frac{C_p' \, W_c}{C_{p4} \, W_t} \right) + TTWIN \left(\frac{C_{pw} \, W_w}{C_{p4} \, W_t} \right)$$

The dry air combustion temperature, TTC, and the specific heat at constant pressure, C_p', are calculated from a propellant performance program at the preheater inlet conditions. The mixture specific heat is calculated in paragraph 28. TTWIN is equal to TT3A.

The augmentor inlet temperature was also monitored with seven thermocouples. However, since the preheater outlet temperature distribution was very nonuniform, the possibility of not obtaining a good average temperature from only seven thermocouples precluded their use in the data reduction routine.

31. Swirl Vane Inlet Mach Number

The swirl vane inlet Mach number is calculated by iterating on the following equation:

$$M_4 = \frac{SVFR(W_a)(1 + HUH + FAPH)}{PT4A(A_4)} \sqrt{\frac{R_4(TT4A)}{GAM4(G)} \left[1 + \frac{GAM4-1}{2} M_4^2\right]^{\frac{GAM4+1}{GAM4-1}}} \tag{37}$$

As before the iteration is carried to the accuracy limit of the computer. The swirl vane inlet area, A_4, is $0.0729 m^2$ ($113.0 in.^2$). The term SVFR is the fraction of the total rig massflow passing through the swirl vanes. The remaining massflow passes through the pilot. An initial value of 0.96 is given to SVFR. After the conditions downstream of the swirl vanes have been determined, a new value of SVFR is calculated. All of the calculations are repeated using the new value of SVFR. This process is repeated until satisfactory convergence between the initial and final values of SVFR is obtained.

32. Augmentor Reference Mach Number

The reference Mach number is calculated by iterating on the following equation:

$$M_{REF} = \frac{W_a(1 + HUM + FAPH)}{PT4A(A_{REF})} \sqrt{\frac{R_4(TT4A)}{GAM4(G)} \left[1 + \frac{GAM4-1}{2} M_{REF}^2\right]^{\frac{GAM4+1}{GAM4-1}}} \tag{38}$$

The iteration is carried to the accuracy limit of the computer. The reference area, A_{REF}, is taken as the annular area between the 0.381 meter (15 in.) diameter outer wall and 0.102 meter (4 in.) diameter centerbody, or $0.1059 m^2$ ($164.15 in.^2$).

33. Augmentor Reference Velocity

The reference velocity is calculated from continuity using the following equation:

$$V_{REF} = W_a(1 + HUM + FAPH)R_4(TT4A)/(PT4A)A_{REF} \tag{39}$$

34. Swirl Vane Inlet Velocity

The gas velocity at the swirl vanes is calculated by continuity as:

$$V_4 = SVFR(W_a)(1 + HUM + FAPH)R_4TT4A/(PT4A)(A_4) \tag{40}$$

35. Nominal Swirl Intensity at the Pilot

The swirl intensity at the pilot is given by:

$$g_s = V_{4T}^2/RG \tag{41}$$

where,

R = Pilot inner wall radius = 0.161 meters (6.33 in.)

G = Standard acceleration due to gravity = 9.805 m/sec^2

$V_{4T} = V_4 * TAN\, \alpha$

36. Swirl Vane Pressure Loss

This pressure loss is given by:

$$DPSV = DPAUG - DPMOM \tag{42}$$

where the total system pressure loss, DPAUG, is given in paragraph 49, and the momentum pressure loss, DPMOM, is given in paragraph 48.

37. Combustion Zone Exit Static Pressure

This pressure is the arithmetic average of two pressures measured with static pressure taps located just ahead of the exhaust nozzle. Therefore:

$$PS5 = (PS51 + PS52)/2 \tag{43}$$

38. Exhaust Total Pressure

The exhaust total pressure is calculated by an iterative procedure. The only known data are the nozzle inlet and throat geometric areas, the augmentor mass-flow and the combustion zone static pressure at the nozzle inlet. The nozzle throat static pressure was taken to be equal to atmospheric pressure for an initial guess. This introduces no error. If the nozzle total pressure is such that the throat Mach number is less than or just equal to 1.0, the throat static pressure is atmospheric. If the nozzle total pressure is any greater, the throat Mach number will be 1.0 and knowledge of the throat static pressure is not necessary.

To start the iteration process the nozzle total pressure is taken to be equal to the measured combustion zone static pressure. The nozzle total temperature is set equal to the ideal total temperature as calculated in paragraph 52. With this data an initial value of the throat Mach number can be calculated as outlined in paragraph 39. Using this Mach number a new value of the gas total temperature is calculated as in paragraph 44. The nozzle throat may or may not be choked. Therefore, using the calculated Mach number the A_{cd}/A^* value at the nozzle throat is given by

$$A_{cd}/A^* = \frac{1}{M_6}\left[\left(\frac{2}{GAM6+1}\right)\left(1+\frac{GAM6-1}{2}M_6^2\right)\right]^{\frac{GAM6+1}{2(GAM6-1)}} \quad (44)$$

where

A^* – Area at a Mach number of unity

A_{cd} Effective area of the exhaust nozzle. (See paragraph 43.)

The specific heat ratio is calculated as in paragraph 45. With this value of A_{cd}/A^* the corresponding value at the nozzle inlet, A_5/A^* is given by

$$A_5/A^* = (A_5/A_{cd})(A_{cd}/A^*) \quad (45)$$

Knowing A_5/A^* the Mach number at the nozzle inlet is found by iterating on the equation:

$$M_5 = \frac{1}{(A_5/A^*)}\left[\left(\frac{2}{GAM6+1}\right)\left(1+\frac{GAM6-1}{2}M_6^2\right)\right]^{\frac{GAM6+1}{2(GAM6-1)}} \quad (46)$$

As before, the iteration is carried to the accuracy limit of the computer. Using this value of the nozzle inlet Mach number a new value of the nozzle total pressure is calculated from

$$PT6A = PS5A\left(1+\frac{GAM6-1}{2}M_5^2\right)^{\frac{GAM6}{GAM6-1}} \quad (47)$$

The iterative procedure involving sections 39, 44 and 52 is repeated until the calculated total temperature converges to within 0.056°C (0.1°F).

The exhaust total pressure was also measured with an exhaust total pressure rake. However, during the course of the program the sensor tips were gradually burned away. This changed the accuracy of the rake over the course of the program. Since more consistent results were obtained with the method described above, it was used for all of the data reduction.

39. Exhaust Mach Number

The exhaust nozzle Mach number is calculated knowing the pressure ratio at the nozzle. Therefore,

$$M_6 = \sqrt{\left(\frac{2}{GAM6-1}\right)\left[\left(\frac{PT6A}{PBAR}\right)^{\frac{GAM6-1}{GAM6}} - 1\right]} \quad (48)$$

Where PBAR is the local atmospheric pressure. The specific heat ratio, GAM6, is calculated in paragraph 45. If the pressure ratio is such that the calculated Mach number is greater than 1.0, the Mach number is set equal to 1.0.

40. Exhaust Nozzle Tangential Mach Number

The tangential Mach number at the exhaust nozzle is used to determine the nozzle discharge coefficient during hot tests. It is calculated by:

$$XMT = V_{T4}\left(\frac{12.66}{D_{noz}}\right) \Big/ \sqrt{GAM6(G)\,(R_6)\,TT6IDEAL} \quad (49)$$

where V_{T4} is given in paragraph 35. The gas constant, R_6, is calculated in paragraph 45. The ideal exit temperature, TT6IDEAL, is calculated in paragraph 52.

41. Exhaust Nozzle Diameter (Cold)

The cold diameter of the exhaust nozzle is an input to the program. Two exhaust nozzles were used in the program. Diameters were 0.272 meters (10.69 in.) and 0.219 meters (8.62 in.).

42. Exhaust Nozzle Discharge Coefficient

The exhaust nozzle discharge coefficient (C_d) is determined using the curve of figure A1. As suggested in Reference 4, the C_d is presented as a function of the tangential Mach number at the nozzle throat (see paragraph 40 for the determination of the throat tangential Mach number) and nozzle pressure ratio.

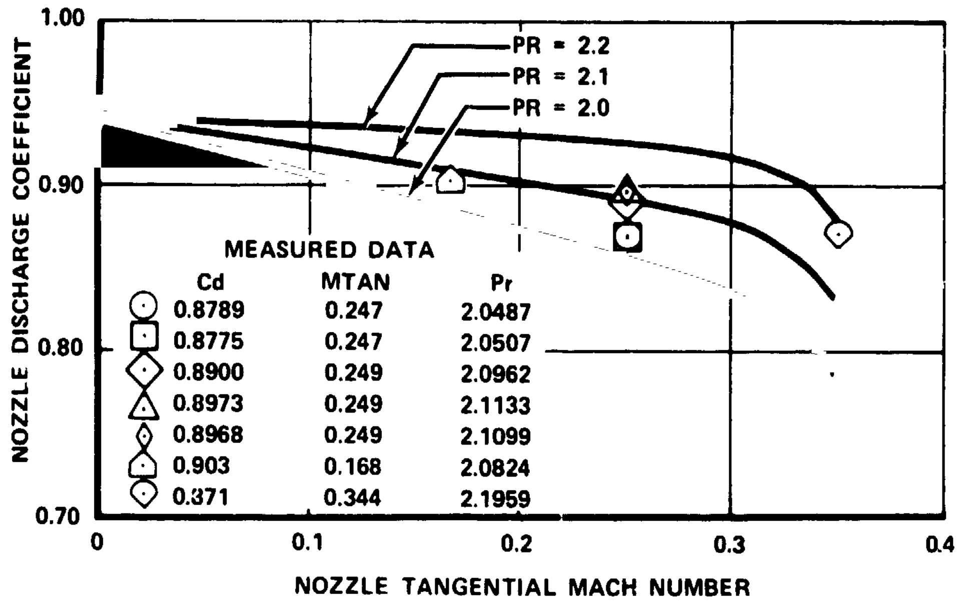

Figure A1. Effect of Pressure Ratio and Tangential Mach Number on Nozzle Discharge Coefficient FD 79974

43. Exhaust Nozzle Effective Area

During cold flow the nozzle effective area is calculated from the isentropic flow relations as follows:

$$A_{cd} = \frac{W_a(1 + HUM + FAPH)}{PT6A(M_6)} \sqrt{\frac{R_6 TT6}{GAM6(G)} \left[1 + \frac{GAM6-1}{2} M_6^2\right]^{\frac{GAM6+1}{GAM6-1}}} \qquad (50)$$

During hot tests the nozzle effective area is calculated by:

$$A_{cd} = C_d A_{noz} \qquad (51)$$

using the appropriate C_d calculated in paragraph 42. The nozzle geometric area is corrected for thermal expansion by the relation:

$$A_{noz} = \frac{\pi}{4} D_{noz}^2 \left[1 + (TNOZA-80)(8.4 \times 10^{-6})\right]^2 \qquad (52)$$

The thermal expansion correction is given by the term in brackets; the nozzle wall temperature is calculated in paragraph 56.

44. Exhaust Gas Total Temperature

Knowing the exhaust nozzle total pressure, effective flow area, exhaust Mach number, and total rig massflow, the exhaust total temperature is given by

$$TT6 = \left[\frac{PT6A(A_{cd})M_6}{W_a(1 + HUM + FAPH + FAO)}\right]^2 \left[\frac{GAM6(G)}{R_6\left(1 + \frac{GAM6-1}{2} M_6^2\right)^{\frac{GAM6+1}{GAM6-1}}}\right] \quad (53)$$

45. Exhaust Gas Gamma

The specific heat ratio, GAM6, for the mixture of air, water and fuel is given by:

$$GAM6 = C_{p6}/(C_{p6} - R_6) \quad (54)$$

The gas constant, R_6, for the mixture is given by:

$$R_6 = \frac{R'(W_a + WFT + WFPH) + R_w W_w}{W_a + WFT + WFPH + W_w} \quad (55)$$

Where R' is a theoretical gas constant obtained from a propellant performance program for the products of combustion at the augmentor operating conditions.

The constant pressure specific heat, C_{p6}, for the mixture is given by:

$$C_{p6} = \frac{C'_p(W_a + WFT + WFPH) + R_w W_w}{W_a + WFT + WFPH + W_w} \quad (56)$$

The specific heat C'_p is obtained from a propellant performance deck at the nozzle exit conditions.

46. Augmentor Temperature Ratio

The temperature ratio across the augmentor is simply:

$$TRATIO = TT6/TT4A \quad (57)$$

47. Pilot Pressure Loss

The pilot system pressure loss is:

$$DPPZ = [(PT4A - PSP)/PT4A]\,100 \quad (58)$$

48. Momentum Pressure Loss

The momentum pressure loss (loss due to combustion) was determined from the relations for simple heating of a perfect gas (Rayleigh line calculation) in a constant area duct. The theoretical total pressure ratio $(P_o/P_o^*)_{M = M_{4.6}}$, if the flow were heated from a state where $M = M_{4.6}$ to a state where $M = 1$, is determined from:

$$\left(\frac{P_o}{P_o^*}\right)_{M = M_{4.6}} \equiv \frac{PT4A}{P_o^*} = \frac{GAM4+1}{1 + GAM4(M_{4.6})^2}\left[\frac{2\left(1 + \frac{GAM4-1}{2} M_{4.6}^2\right)}{GAM4+1}\right]^{\frac{GAM4}{GAM4-1}} \qquad (59)$$

The Mach number, $M_{4.6}$, is evaluated at the plane of the zone 2, 3 and 4 spraybars using the temperature and pressure conditions at the swirl vane inlet. The Mach number calculation is identical to that outlined in paragraph 32 for the reference Mach number. The only difference is the area which is taken as the chamber cross-section at the plane of the spraybars or 0.114m^2 (176.7 in.^{2}). The theoretical total temperature ratio, $(T_o/T_o^*)_{M = M_{4.6}}$, if the flow were heated from a state where $M = M_{4.6}$ to a state where $M = 1$, is determined from:

$$\left(\frac{T_o}{T_o^*}\right)_{M = M_{4.6}} \equiv \frac{TT4A}{T_o^*} = 2\,(GAM4+1)\,M_{4.6}^2\left[\frac{1 + \frac{GAM4-1}{2} M_{4.6}^2}{(1 + GAM4(M_{4.6}^2))^2}\right] \qquad (60)$$

Knowing the exhaust total temperature and hence the exhaust-to-inlet temperature ratio, TT6/TT4A, the Mach number M_5 just upstream of the exhaust nozzle is calculated from:

$$\frac{TT4A}{T_o^*} \times \frac{TT6}{TT4A} = \frac{TT6}{T_o^*} = 2(GAM6+1)M_5^2 \left[\frac{1 + \frac{GAM6-1}{2} M_5^2}{(1 + GAM6-1(M_5^2))^2} \right] \qquad (61)$$

Using Mach number, M_5, and the pressure ratio PT4A/P_o^* computed in equation 59, the total pressure just upstream of the exhaust nozzle is then determined from:

$$\frac{PT5IDEAL}{PT4A} \times \frac{PT4A}{P_o^*} =$$

$$\frac{PT5IDEAL}{P_o^*} = \frac{GAM6+1}{1 + GAM6(M_5)^2} \left[\frac{2\left(1 + \frac{GAM6-1}{2} M_5^2\right)}{GAM6+1} \right]^{\frac{GAM6}{GAM6-1}} \qquad (62)$$

The momentum pressure loss is then:

$$DPMOM = \left(\frac{PT4A - PT5IDEAL}{PT4A} \right) 100 \qquad (63)$$

49. Total System Pressure Loss

The total system pressure loss is simply:

$$DPAUG = \left(\frac{PT4A - PT6A}{PT4A} \right) 100 \qquad (64)$$

50. Preheater Fuel-to-Air Ratio

The preheater fuel-to-air ratio is simply:

$$FAPH = WFPH/(3600\ W_a) \qquad (65)$$

51. Preheater Efficiency

The preheater efficiency is given by:

$$EFFPH = (TT4A - TT3A)/(TT4IDEAL - TT3A) \qquad (66)$$

The ideal preheater outlet temperature, TT4IDEAL, is given in paragraph 30.

52. Ideal Exhaust Total Temperature

The ideal exhaust total temperature is calculated in the same manner as the preheater ideal temperature. The ideal dry exhaust total temperature is calculated from the propellant performance program as the temperature that would result from combustion of dry air at the preheater inlet temperature TT3A and the total rig fuel flow (stand preheater fuel, pilot fuel, and main combustion zone fuel). This temperature is then corrected for water vapor in the inlet airflow as follows. From an enthalpy balance:

$$H_6 - H_{win} + H_a + H_f \quad H_{win} + H_c$$

Note once again that the enthalpy of the water is considered constant. The enthalpies used in the above equation are total enthalpies, which include the kinetic energy associated with each component. Thus:

$$W_T C_{p6}\, TT6IDEAL - W_w C_{pw}\, TTWIN + W_c C'_p\, TTC$$

Rearranging:

$$TT6IDEAL \quad TTC\left(\frac{C'_p W_c}{C_{p6} W_T}\right) + TTWIN\left(\frac{C_{pw} W_w}{C_{p6} W_T}\right) \tag{67}$$

C'_p, the specific heat of the dry combustion products is determined from the propellant performance program. The specific heat for the mixture, C_{p6}, is determined as outlined earlier for air, water, and fuel mixtures (paragraph 45). As before, TTWIN is equal to TT3A.

53. Augmentor Efficiency

The augmentor combustion efficiency is given by:

$$EFFMB \quad \left[\left(\frac{TT6 - TT4A}{TT6IDEAL - TT4A}\right) + \frac{3600\, Q_{loss}}{18370\, W_{FT}}\right] 100 \tag{68}$$

The cooling water heat loss, Q_{loss}, is calculated in Section 17.

Equation (68) calculates the augmentor efficiency by comparing the ideal temperature rise to the actual temperature rise as determined from the calculated value of TT6. For a portion of the tests the combustion efficiency was also determined by sampling the exhaust gases for unburned hydrocarbons and carbon monoxide. The combustion efficiency is then given by:

$$\text{EFFMB} = 100 - 100 \; \frac{\text{HVco(CO)} + \text{HVf(UHC)}}{\text{HVf} \times 10^3} \tag{69}$$

where

CO = emission index of carbon monoxide

UHC = emission index of unburned hydrocarbons

HVco = heating value of carbon monoxide = 1.010×10^7 Joules/kg (4343 Btu/lb_m)

HVf = heating value of the fuel = 4.273×10^7 Joules/kg (18,370 Btu/lb_m)

54. Drag Coefficient - Vane Mach Number

The augmentor drag coefficient based on the swirl vane inlet Mach number is:

$$\text{CDAUG} = (\text{PT4A} - \text{PT6A})/Q_4 \tag{70}$$

Where the dynamic head Q_4 is given by:

$$Q_4 = \frac{\text{GAM4(PT4A)}M_4^2}{2\left[1 + \frac{\text{GAM4-1}}{2} M_4^2\right]^{\frac{\text{GAM4}}{\text{GAM4-1}}}} \tag{71}$$

55. Drag Coefficient - Reference Mach Number

The augmentor drag coefficient based on reference Mach number is:

$$\text{CDREF} = (\text{PT4A} - \text{PT6A})/Q_{REF} \tag{72}$$

Where

$$Q_{REF} = \frac{\text{GAM4(PT4A)}M_{REF}^2}{2\left[1 + \frac{\text{GAM4-1}}{2} M_{REF}^2\right]^{\frac{\text{GAM4}}{\text{GAM4-1}}}} \tag{73}$$

56. Exhaust Nozzle Average Skin Temperature

The nozzle throat skin temperature is an arithmetic average of 4 chromel-alumel skin thermocouples or:

$$TNOZA = \sum_{I=1}^{4} TNOZ(I)/4 \qquad 74$$

APPENDIX B
LIST OF SYMBOLS

A_1	-	Orifice upstream area
A_2	-	Orifice throat area
A_4	-	Swirl vane inlet area, 729 cm^2 (113.0 $in.^2$)
$A_{4.5}$	-	Flow area upstream of the swirl vanes, 1380 cm^2 (214.4 $in.^2$)
$A_{4.6}$	-	Flow area at the sprayrings, 1140 cm^2 (176.6 $in.^2$)
A_5	-	Flow area at the nozzle inlet, 1140 cm^2 (176.6 $in.^2$)
A_{cd}	-	Nozzle throat effective area
A_{noz}	-	Nozzle geometric area
A_p	-	Pilot zone inlet area, 24.47 cm^2 (3.79 $in.^2$)
A_{ref}	-	Augmentor reference area, 1059 cm^2 (164.15 $in.^2$)
A^*	-	Flow area at Mach number equal 1.0
BAFDP	-	Back-up orifice delta pressure
BAFP1	-	Back-up orifice upstream pressure
BAFTTA	-	Back-up orifice average temperature
C_d	-	Nozzle discharge coefficient
CDAUG	-	Augmentor drag coefficient based on swirl vane inlet Mach number
CDREF	-	Augmentor drag coefficient based on reference Mach number
C_f	-	Ratio of computed flow using wet gas properties to that using dry gas properties
C_{pa}	-	Specific heat at constant pressure for dry air
C_{pm}	-	Specific heat at constant pressure for a mixture of dry air and water vapor
C_{pw}	-	Specific heat at constant pressure for water vapor
C_{p4}	-	Specific heat at constant pressure for a mixture of water vapor and combustion products at the swirl vane inlet

C_{p6}	-	Specific heat at constant pressure for a mixture of water vapor and combustion products at the nozzle exit
C_p'	-	Specific heat at constant pressure for dry combustion products
DNOZ	-	Nozzle diameter - cold
DPAUG	-	Augmentor total pressure loss
DPFPZ	-	Pilot zone fuel pressure drop
DPFZ2	-	Zone 2 fuel pressure drop
DPFZ3	-	Zone 3 fuel pressure drop
DPFZ4	-	Zone 4 fuel pressure drop
DPMOM	-	Momentum pressure drop (pressure drop due to heating)
DPORF	-	Primary airflow orifice pressure drop
DPPZ	-	Pilot zone air pressure loss
DPSV	-	Swirl vane pressure loss
DP_W	-	Pressure drop across cooling water flow measuring orifice
EFFMB	-	Augmentor combustion efficiency
EFFPH	-	Preheater combustion efficiency
FA2	-	Augmentor fuel/air ratio due to zone 2 fuel flow
FA3	-	Augmentor fuel/air ratio due to zone 3 fuel flow
FA4	-	Augmentor fuel/air ratio due to zone 4 fuel flow
FAO	-	Augmentor fuel/air ratio
FAPH	-	Preheater fuel/air ratio
FAPZ	-	Pilot zone fuel/air ratio
G	-	Standard acceleration due to gravity
GAM4	-	Specific heat ratio at swirl vane inlet
GAM6	-	Specific heat ratio at nozzle exit

g_s	-	Swirl intensity at the pilot inner wall, defined in Equation (41)
H_a	-	Enthalpy of entering air
H_c	-	Enthalpy of combustion products
H_f	-	Enthalpy of fuel including heat of combustion
H_4	-	Enthalpy of gas at swirl vane inlet
H_6	-	Enthalpy of gas at nozzle exit
HUM	-	Specific humidity of entering air
HWIN	-	Enthalpy of entering water vapor
L	-	Combustion zone length
L/D	-	Combustion zone length-to-diameter ratio
M_4	-	Swirl vane inlet Mach number
$M_{4.5}$	-	Mach number just upstream of the swirl vanes
$M_{4.6}$	-	Mach number at the plane of the fuel sprayrings
M_5	-	Exhaust nozzle inlet Mach number
M_6	-	Nozzle exit Mach number
M_{pz}	-	Mach number through pilot swirler
M_{ref}	-	Augmentor reference Mach number
P_1	-	Orifice upstream pressure
P_2	-	Orifice throat pressure
PBAR	-	Atmospheric pressure
PFPZ	-	Pilot zone fuel pressure
PFZ2	-	Zone 2 fuel pressure
PFZ3	-	Zone 3 fuel pressure
PFZ4	-	Zone 4 fuel pressure
P_o^*	-	Total pressure at Mach number unity
PORF1	-	Primary orifice upstream pressure
I	-	Total to static pressure ratio

PS4.5	-	Static pressure just upstream of swirl vanes
PS5A	-	Nozzle inlet static pressure
PSP	-	Pilot zone static pressure
PT4A	-	Augmentor inlet total pressure
PT5IDEAL	-	Ideal total pressure at nozzle inlet
PT6A	-	Exhaust nozzle total pressure
Q_4	-	Swirl vane dynamic head
Q_{loss}	-	Heat rejected to cooling water
Q_{REF}	-	Reference dynamic head
R	-	Pilot inner wall radius
R_a	-	Gas constant for dry air
R_m	-	Gas constant for a mixture of dry air and water vapor
R_w	-	Gas constant for water vapor
R_4	-	Gas constant at the swirl vane inlet
R_6	-	Gas constant at the nozzle exit
R'	-	Gas constant for the dry combustion products
SVFR	-	Fraction of total rig massflow passing through the swirl vanes
TNOZA	-	Exhaust nozzle wall temperature
T_c^*	-	Total temperature at Mach number unity
TORF	-	Primary orifice temperature
TRATIO	-	Ratio of outlet to inlet temperature
TT3A	-	Preheater inlet total temperature
TT4A	-	Rig inlet total temperature
TT4IDEAL	-	Ideal preheater outlet temperature
TT6	-	Augmentor outlet total temperature
TT6IDEAL	-	Ideal augmentor outlet temperature

TTC	-	Ideal combustion temperature-dry
TTWIN	-	Temperature of entering water vapor
TWIN	-	Cooling water inlet temperature
TWORF	-	Cooling water outlet temperature
V_4	-	Swirl vane inlet velocity
V_{4T}	-	Tangential velocity at the pilot inner wall
V_{REF}	-	Reference velocity
W_a	-	Dry airflow rate
W_c	-	Dry flowrate of combustion products
WCW	-	Cooling water flowrate
WFPZ	-	Pilot zone fuel flow
WFT	-	Total augmentor fuel flow
WFZ2	-	Zone 2 fuel flow
WFZ3	-	Zone 3 fuel flow
WFZ4	-	Zone 4 fuel flow
W_{pz}	-	Pilot zone airflow
WT	-	Total massflow at the exhaust nozzle
W_w	-	Water vapor flowrate
XMT	-	Tangential Mach number at the exhaust nozzle exit
α	-	Swirl vane angle
γ_a	-	Specific heat at constant pressure of dry air
γ_m	-	Specific heat at constant pressure of water vapor and dry air
ϕ	-	Augmentor equivalence ratio
ϕ_2	-	Zone 2 equivalence ratio
ϕ_3	-	Zone 3 equivalence ratio
ϕ_4	-	Zone 4 equivalence ratio
ρ_w	-	Cooling water density

REFERENCES

1. Schwartz, I. R., "A Preliminary Investigation of Combustion with Rotating Flow in an Annular Combustion Chamber." NACA RML51E25a, 1951.

2. Lewis, G. D., "Centrifugal Force Effects on Combustion," Proceedings of the XIVth Symposium on Combustion, Pennsylvania State University, 1972.

3. Mestre, A., "Efficiency and Pollutant Formation Studies in a Swirling Flow Combustor," Joint Fluids Engineering and CSME Conference, Montreal, Quebec, May 13-15, 1974.

4. Boerner, C. J., E. M. Sparrow, and C. J. Scott, "Compressible Swirling Flow Through Convergent-Divergent Nozzles," Waerme-und Stoffuebertragung, V5n2, P. 101-115, 1972.